

The connectivity of the human frontal pole cortex, and a theory of its involvement in exploit versus explore

Edmund T. Rolls^{1,2,3,*}, Gustavo Deco^{4,5,6}, Chu-Chung Huang^{7,8}, Jianfeng Feng^{2,3}

¹Oxford Centre for Computational Neuroscience, Oxford, United Kingdom,

²Department of Computer Science, University of Warwick, Coventry CV4 7AL, United Kingdom,

³Instituto de Ciencia and Tecnología for Brain Inspired Intelligence, Fudan University, Shanghai 200403, China,

⁴Center for Brain and Cognition, Computational Neuroscience Group, Department of Information and Communication Technologies, Universitat Pompeu Fabra, Roc Boronat 138, Barcelona 08018, Spain,

⁵Brain and Cognition, Pompeu Fabra University, Barcelona 08018, Spain,

⁶Institució Catalana de la Recerca i Estudis Avançats (ICREA), Universitat Pompeu Fabra, Passeig Lluís Companys 23, Barcelona 08010, Spain,

⁷Shanghai Key Laboratory of Brain Functional Genomics (Ministry of Education), Institute of Brain and Education Innovation, School of Psychology and Cognitive Science, East China Normal University, Shanghai 200602, China,

⁸Shanghai Center for Brain Science and Brain-Inspired Technology, Shanghai 200602, China

*Corresponding author: Department of Computer Science, University of Warwick, Coventry CV4 7AL, United Kingdom. Email: Edmund.Rolls@oxcns.org, <https://www.oxcns.org>

The frontal pole is implicated in humans in whether to exploit resources versus explore alternatives. Effective connectivity, functional connectivity, and tractography were measured between six human frontal pole regions and for comparison 13 dorsolateral and dorsal prefrontal cortex regions, and the 360 cortical regions in the Human Connectome Project Multi-modal-parcellation atlas in 171 HCP participants. The frontal pole regions have effective connectivity with Dorsolateral Prefrontal Cortex regions, the Dorsal Prefrontal Cortex, both implicated in working memory; and with the orbitofrontal and anterior cingulate cortex reward/non-reward system. There is also connectivity with temporal lobe, inferior parietal, and posterior cingulate regions. Given this new connectivity evidence, and evidence from activations and damage, it is proposed that the frontal pole cortex contains autoassociation attractor networks that are normally stable in a short-term memory state, and maintain stability in the other prefrontal networks during stable exploitation of goals and strategies. However, if an input from the orbitofrontal or anterior cingulate cortex that expected reward, non-reward, or punishment is received, this destabilizes the frontal pole and thereby other prefrontal networks to enable exploration of competing alternative goals and strategies. The frontal pole connectivity with reward systems may be key in exploit versus explore.

Key words: prefrontal cortex; frontal pole; effective connectivity; exploit versus explore; human connectome; attractor network.

Introduction

The connectivity and functions of the human frontal polar cortex, Area 10, are relatively unknown. Shallice and colleagues found that patients with frontal pole damage had problems optimizing a plan to visit many shops in an efficient order, and more generally had disorganized behavior (Shallice and Burgess 1991; Shallice and Cipolotti 2018). These patients also have deficits in tasks that require abstract reasoning, problem-solving, or multitasking (Hogeveen et al. 2022a). In humans, the frontal pole is activated by tasks that require cognitive branching, value-based decision-making, and metacognition (Hogeveen et al. 2022a). These are tasks that require appropriate action to two or more competing goals (Averbeck 2015; Mansouri et al. 2017a; Mansouri et al. 2017b; Hogeveen et al. 2022a; Hogeveen et al. 2022b). The frontal pole in humans is activated by counterfactual choice tasks with the frontal pole sensitive to the value of unchosen or alternative options during decision-making (Hogeveen et al. 2022a). Consistent with this, in a foraging task, the frontal pole cortex is implicated in whether to exploit what is currently available, or to explore other options in case greater rewards might be available (Hogeveen et al. 2022b). Stimulation of the frontal pole has been tried as a treatment for obsessive-compulsive disorder (which

might be related to too little exploration), and for depression (Hanlon et al. 2021). However, relatively little is known of the connectivity of the human frontal pole cortex except with diffusion tractography (DTI) (Catani et al. 2012; Thiebaut de Schotten et al. 2012; Rojkova et al. 2016). In macaques, connections from superior temporal cortex auditory regions, from dorsolateral prefrontal cortex (Areas 9 and 46), and orbitofrontal cortex have been described (Schmahmann and Pandya 2006; Medalla and Barbas 2010; Petrides et al. 2012; Yeterian et al. 2012; Markov et al. 2014; Medalla and Barbas 2014; Barbas 2015; Hogeveen et al. 2022a), and in humans a frontal orbito-polar tract has been described with DTI connecting BA11 and BA25 with the frontal pole (BA 10) (Catani et al. 2012; Thiebaut de Schotten et al. 2012; Rojkova et al. 2016).

In this context, and given the great development and heterogeneity of functions of different parts of the human prefrontal cortex, and the importance of evidence about the connectivity of different cortical regions for understanding brain computations (Rolls 2000; Rajalingham et al. 2018; Zhuang et al. 2021; Rolls 2021a, 2021c; Rolls 2023a), the aim of the present investigation is to advance understanding of the connections and connectivity of the human frontal pole cortex.

To do this, we measured with Human Connectome Project data (Glasser et al. 2016b) the direct connections of frontal pole cortical regions using diffusion tractography; the functional connectivity between cortical regions using the correlation between the BOLD signals in resting state fMRI that provides evidence about the strength of interactions; and the effective connectivity which provides evidence about the strength and direction of the causal connectivity between pairs of hundreds of cortical regions measured with a new Hopf algorithm (Rolls et al. 2022a, 2022b, 2023d, 2023c). The algorithm measures “generative effective connectivity,” in that it is the strength of the effective connectivity in both directions between all the cortical regions (nodes) that generates the functional connectivity, and the functional connectivity between the nodes when delayed by a short time (τ seconds defined below) to reflect the directionality (Rolls et al. 2023f). These measures were made between the 360 cortical regions in the Human Connectome Project multimodal parcellation atlas (HCP-MMP) (Glasser et al. 2016a). The HCP-MMP atlas was chosen because it provides the most detailed parcellation of the human cortical areas that we know, in that its 360 cortical regions are defined using a multimodal combination of structural measures (cortical thickness and cortical myelin content), functional connectivity, and task-related fMRI (Glasser et al. 2016a). This parcellation is the parcellation of choice for the cerebral cortex because it is based on multimodal information (Glasser et al. 2016a) with the definitions and boundaries set out in their Glasser_2016_SuppNeuroanatomy.pdf, and it is being used as the basis for many new investigations of brain function and connectivity, which can all be cast in the same framework (Colclough et al. 2017; Van Essen and Glasser 2018; Sulpizio et al. 2020; Huang et al. 2021; Yokoyama et al. 2021; Ma et al. 2022; Rolls et al. 2022a, 2022b, 2023a, 2023b, 2023c, 2023d, 2023e, 2023g, 2023h). This approach provides better categorization of cortical areas than does for example functional connectivity alone (Power et al. 2011). A summary of the boundaries, tractography, functional connectivity, and task-related activations of frontal cortical areas using the HCP-MMP atlas is available elsewhere (Glasser et al. 2016a; Baker et al. 2018a, 2018b, 2018c, 2018d, 2018e), but the effective connectivity, tractography, and functional connectivity analyses described here are new, and further are presented in quantitative form using connectivity matrices for all 360 cortical areas.

All of the area 10 cortical regions in the HCP-MMP atlas were included in this investigation. The main frontal pole area 10 regions are 10d, 10 pp, a10p, and p10p (see Fig. 1). However, we also included the other two area 10 regions, 10r and 10v, but as they extend further posterior they are shown separately above the first red line in the cortical connectivity diagrams. We quickly found that the frontal pole regions have extensive connectivity with dorsolateral prefrontal cortex (DLPFC) areas (in the DLPFC division in the HCP-MMP atlas, as shown in Table S1), and much less with the regions in the inferior frontal gyrus division. We therefore thought it important to compare in the Figures in this investigation the connectivity of frontal pole regions with those of DLPFC regions, to elucidate how different the connectivity may be of the human frontal pole area 10 cortex from that of the dorsolateral prefrontal cortex. The dorsolateral prefrontal cortex regions are implicated in short-term memory (Funahashi et al. 1989; Goldman-Rakic 1996; Goldman and Leung 2002) by maintaining firing in an attractor network (Martinez-Garcia et al. 2011; Fuster 2015; Constantinidis et al. 2018; Lundqvist et al. 2018; Rolls 2023a). These prefrontal cortex regions are thereby involved in working memory and executive function (Baddeley 2012;

Miller 2013; Miller et al. 2018; Baddeley et al. 2019; Baddeley 2021; Fuster 2021; Passingham 2021) and top-down attention (Deco and Rolls 2004, 2005a, 2005b; Rolls 2023a).

The effective and functional connectivity of the frontal pole regions and the dorsal and dorsolateral prefrontal cortex regions considered here was measured in the resting state in 171 HCP participants at 7T, because this connectivity provides a starting point for the analysis of brain connectivity when it is not influenced by particular tasks. Moreover, this means that the connectivities described here can be compared directly with those of other cortical regions described in other research using the same analyses (Ma et al. 2022; Rolls et al. 2022a, 2022b, 2023a, 2023b, 2023d, 2023c, 2023e, 2023g, 2023h). However, the connectivities described here were found to be almost identical in 956 HCP participants imaged in the resting state at 3T. Moreover, the connectivities described here were also shown to be generically similar in the HCP visual working memory task (Barch et al. 2013), though they are modulated by whether faces, places, etc., are being presented. Moreover, the differences of effective connectivity in the forward and reverse directions were in the same direction as described here, though smaller, during the visual working memory task. In the descriptions provided here, some distinction is made because of their different connectivities between regions such as 46, 9-46d, a9-46v, and p9-46v in the dorsolateral prefrontal cortex (DLPFC), and regions 8Ad, 8Av, 8BL, 8C, 9a, 9b, and 9m, which are dorsal prefrontal cortex regions (Passingham 2021).

The present research goes beyond previous research by estimating causal, effective, connectivity between 19 frontal cortical regions in the human brain with the HCP multimodal atlas with 360 cortical areas. Strengths of this investigation are that it utilized this surface-based HCP-MMP atlas (Glasser et al. 2016a); HCP data from 171 participants imaged in the resting state at 7T (Glasser et al. 2016b) in whom we could calculate the functional connectivity and effective connectivity in the surface-based HCP-MMP atlas; and that it utilized a method for effective connectivity measurement between all 360 cortical regions investigated here. The Hopf effective connectivity algorithm is important for helping to understand the operation of the computational systems in the brain, for it is calculated using time delays in the signals between 360 or more cortical regions (Rolls et al. 2022a, 2022b, 2023c, 2023d), and the use of time is an important component in the approach to causality (Rolls 2021d). We hope that future research using the same brain atlas (Glasser et al. 2016a; Huang et al. 2022) will benefit from the human frontal cortical and related connectome described here. In a previous investigation, the connectivity of the dorsolateral prefrontal cortex was measured in 171 HCP participants imaged at 7T in the resting state (Rolls et al. 2023e). The present investigation is different, in that it focuses on the effective connectivity, functional connectivity, and diffusion tractography of the frontal pole not considered in that or any other previous investigation.

Methods

Participants and resting state fMRI data acquisition

Multiband 7T resting state functional magnetic resonance images (rs-fMRI) of 184 individuals were obtained from the publicly available S1200 release (last updated: April 2018) of the Human Connectome Project (HCP) (Van Essen et al. 2013). Individual written informed content was obtained from each participant, and the scanning protocol was approved by the Institutional Review Board of Washington University in St. Louis, MO, USA (IRB #201204036).

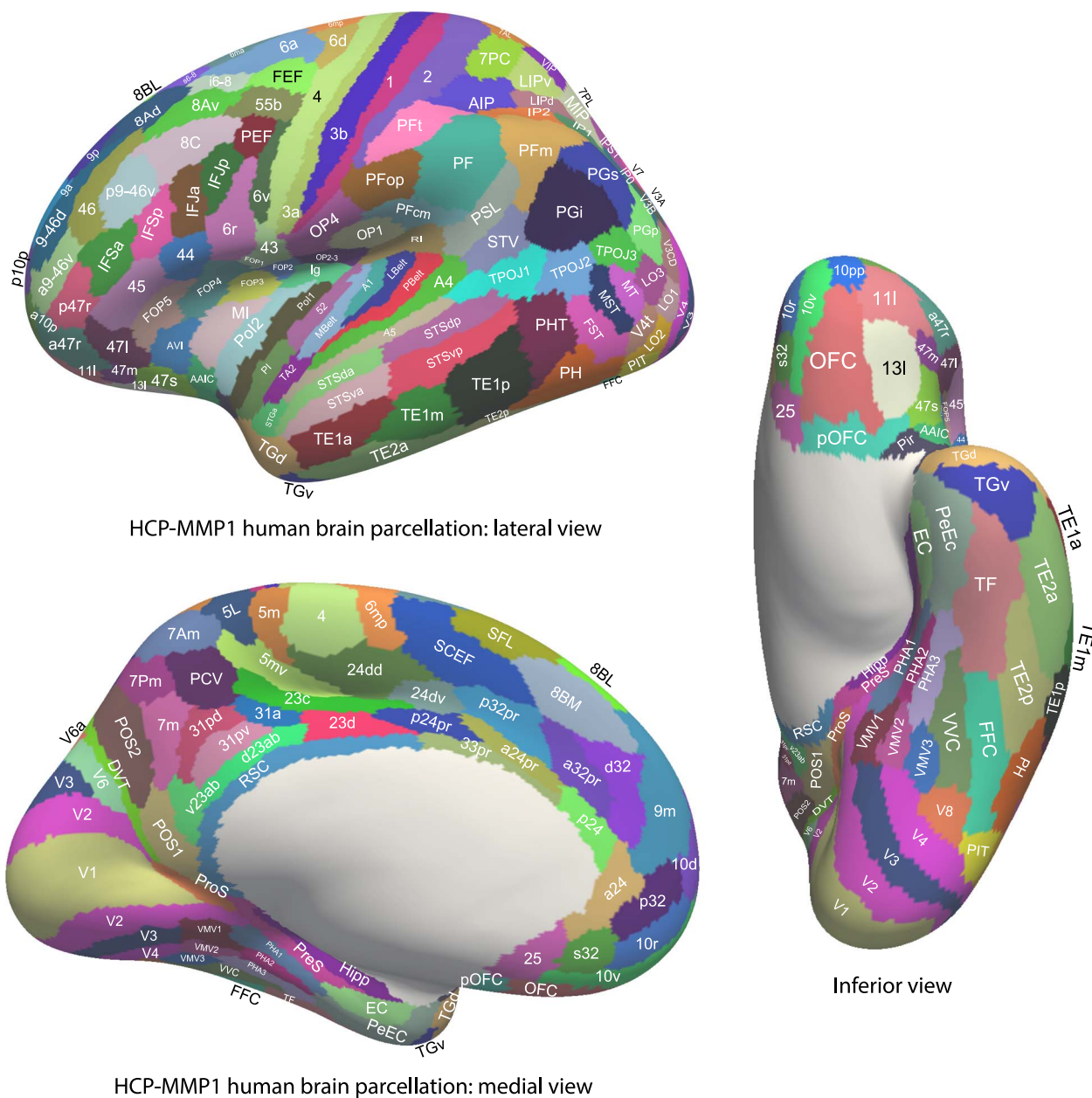


Fig. 1. Regions in the human connectome project multimodal Parcellation atlas (HCP-MMP) (Glasser et al. 2016a) and its extended version HCPex (Huang et al. 2022) to show the frontal cortex regions analyzed here. The regions are shown on images of the human brain with the sulci expanded sufficiently to allow the regions within the sulci to be shown. Abbreviations are provided in Table S1. For comparison, a version of this diagram without the sulci expanded is provided in Figs. S1-5.

Multimodal imaging was performed in a Siemens Magnetom 7T housed at the Center for Magnetic Resonance (CMRR) at the University of Minnesota in Minneapolis. For each participant, a total of four sessions of rs-fMRI were acquired, with oblique axial acquisitions alternated between phase encoding in a posterior-to-anterior (PA) direction in sessions 1 and 3, and an anterior-to-posterior (AP) phase encoding direction in sessions 2 and 4. Specifically, each rs-fMRI session was acquired using a multiband gradient-echo EPI imaging sequence. The following parameters were used: TR = 1,000 ms, TE = 22.2 ms, flip angle = 45°, field of view = 208 × 208, matrix = 130 × 130, 85 slices, voxel size = 1.6 × 1.6 × 1.6 mm³, multiband factor = 5. The total scanning time for the rs-fMRI protocol was ~16 min with 900 volumes. Further details of the 7T rs-fMRI acquisition protocols are given

in the HCP reference manual (https://humanconnectome.org/storage/app/media/documentation/s1200/HCP_S1200_Release_Reference_Manual.pdf).

The current investigation was designed to complement investigations of effective and functional connectivity and diffusion tractography of the hippocampus (Huang et al. 2021; Ma et al. 2022; Rolls et al. 2022b), posterior cingulate cortex (Rolls et al. 2023h), parietal cortex (Rolls et al. 2023d), orbitofrontal, ventromedial prefrontal, and anterior cingulate cortex (Rolls et al. 2023a, 2023c), language cortical regions (Rolls et al. 2022a), visual cortical regions (Rolls et al. 2023b), posterior parietal cortex regions (Rolls et al. 2023d), prefrontal and somatosensory regions (Rolls et al. 2023e), and auditory cortex regions (Rolls et al. 2023g), by extending the analysis to the frontal pole

cortex using the same analysis methods as in these previous investigations.

Data preprocessing

The preprocessing was performed by the HCP as described in Glasser et al. (2013), based on the updated 7T data pipeline (v3.21.0, https://github.com/Washington-University/HCP_pipelines), including gradient distortion correction, head motion correction, image distortion correction, spatial transformation to the Montreal Neurological Institute space using one step spline resampling from the original functional images followed by intensity normalization. In addition, the HCP took an approach using ICA (FSL's MELODIC) combined with a more automated component classifier referred to as FIX (FMRIB's ICA-based X-noisifier) to remove non-neural spatiotemporal artifact (Smith et al. 2013; Griffanti et al. 2014; Salimi-Khorshidi et al. 2014). This step also used 24 confound timeseries derived from the motion estimation (six rigid-body parameter timeseries, their backwards-looking temporal derivatives, plus all 12 resulting regressors squared (Satterthwaite et al. 2013) to minimize noise in the data. The preprocessing performed by the HCP also included boundary-based registration between EPI and T1w images, and brain masking based on FreeSurfer segmentation. The "minimally preprocessed" rsfMRI data provided by the HCP 1200 release (rfMRI*hp2000_clean.dtseries) was used in this investigation. The preprocessed data is in the HCP grayordinates standard space and is made available in a surface-based CIFTI file for each participant. With the MATLAB script (cifti toolbox: <https://github.com/Washington-University/cifti-matlab>), we extracted and averaged the cleaned timeseries of all the grayordinates in each region of the HCP-MMP 1.0 atlas (Glasser et al. 2016a), which is a group-based parcellation defined in the HCP grayordinate standard space having 180 cortical regions per hemisphere, and is a surface-based atlas provided in CIFTI format. The timeseries were detrended, and temporally filtered with a second order Butterworth filter set to 0.008–0.08 Hz.

Brain atlas and region selection

To construct the effective connectivity for the regions of interest in this investigation with other parts of the human brain, we utilized the 7T resting state fMRI HCP data, and parcellated this with the surface-based HCP-MMP atlas which has 360 cortical regions (Glasser et al. 2016a). We were able to use the same 171 participants for whom we also had performed diffusion tractography, as described in detail (Huang et al. 2021). The brain regions in this atlas (Glasser et al. 2016a) are shown in Figs. 1 and S1, and a list of the cortical regions in this atlas and the divisions into which they are placed is provided in Table S1 in the reordered form used in the extended volumetric HCPex atlas (Huang et al. 2022).

The 19 frontal pole and related cortical regions selected for connectivity analysis here were as follows, in the HCP-MMP division indicated (and set out in Table S1) where relevant. We started by selecting the four key area 10 regions at the frontal pole, 10d, 10p, 10pp, a10p, and p10p (see Fig. 1). To these we added a second set of regions, 10r and 10v, parts of which are at the frontal pole, and parts of which extend posteriorly into what is sometimes terms the ventromedial prefrontal cortex, vmPFC (Rolls et al. 2023c) (see Fig. 1). A third set of regions included for comparison with frontal pole regions were the Dorsal Prefrontal regions (Passingham 2021) 8Ad, 8Av, 8BL, 8C, 9a, 9p, 9m and intermediate regions i6–8 and s6–8. A fourth set of regions also included for comparison were the Dorsolateral Prefrontal Cortex (Passingham 2021) regions 46, 9-46d, a9-46v, and p9-46v. In the figures in this paper, red lines

separate the four sets of regions, to facilitate comparison of the connectivity of these four sets of regions. Although the connectivity of some of these regions has been described previously (Rolls et al. 2023c, 2023e), the connectivity of the frontal pole regions has not been considered previously, nor compared with that of other frontal cortex regions, so that the frontal pole connectivity analyses described here are new. Background on the boundaries and activations found in each of the brain regions considered here is provided elsewhere (Glasser et al. 2016a; Baker et al. 2018a, 2018b, 2018e).

It is noted that the HCP-MMP atlas sometimes uses dorsal versus ventral as descriptors following nomenclature in non-human primates, and that these correspond to superior and inferior in humans. For those becoming familiar with the HCP-MMP atlas, in the name of a cortical region, typically a = anterior, p = posterior, d = dorsal (i.e. superior in the human brain), v = ventral (i.e. inferior in the human brain), m = medial, l or L = lateral, T = temporal, P = parietal, and V = visual. It must also be noted that some of the names used in the HCP-MMP atlas utilize the name of the corresponding region in macaques, but in humans the cortical region may not be topologically in the same place (e.g. sulcus) as in macaques.

Measurement of effective connectivity

Effective connectivity measures the effect of one brain region on another, and utilizes differences detected at different times in the signals in each connected pair of brain regions to infer effects of one brain region on another. One such approach is dynamic causal modeling, but it applies most easily to activation studies, and is typically limited to measuring the effective connectivity between just a few brain areas (Friston 2009; Valdes-Sosa et al. 2011; Bajaj et al. 2016), though there have been moves to extend it to resting state studies and more brain areas (Frassle et al. 2017; Razi et al. 2017). The method used here (see Rolls et al. 2022b, 2023c) was developed from a Hopf algorithm to enable measurement of effective connectivity between many brain areas, described by Deco et al. (2019). A principle is that the functional connectivity is measured at time t and time $t + \tau$, where τ is typically 2 s to take into account the time within which differences in the timing of the BOLD signal can be detected, and that τ should be short to capture causality, and then the effective connectivity model is trained by error correction until it can generate the functional connectivity matrices at time t and time $t + \tau$. Further details of the algorithm, and the development that enabled it to measure the effective connectivity in each direction, are described next and in more detail in the [Supplementary Material](#).

To infer the effective connectivity, we use a whole-brain model that allows us to simulate the BOLD activity across all brain regions and time. We use the so-called Hopf computational model, which integrates the dynamics of Stuart-Landau oscillators, expressing the activity of each brain region (Deco et al. 2017b). As mentioned above, we include in the model 360 cortical brain areas (Huang et al. 2022). The local dynamics of each brain area (node) is given by Stuart-Landau oscillators which expresses the normal form of a supercritical Hopf bifurcation, describing the transition from noisy to oscillatory dynamics (Kuznetsov 2013). During the last years, numerous studies were able to show how the Hopf whole-brain model successfully simulates empirical electrophysiology (Freyer et al. 2011; Freyer et al. 2012), MEG (Deco et al. 2017a) and fMRI (Kringelbach et al. 2015; Deco et al. 2017b; Kringelbach and Deco 2020).

The Hopf whole-brain model can be expressed mathematically as follows:

$$\frac{dx_i}{dt} = \underbrace{[a_i - x_i^2 - y_i^2]x_i - \omega_i y_i}_{\text{Local Dynamics}} + \underbrace{G \sum_{j=1}^N C_{ij} (x_j - x_i)}_{\text{Coupling}} + \underbrace{\beta \eta_i(t)}_{\text{Gaussian Noise}} \quad (1)$$

$$\frac{dy_i}{dt} = [a_i - x_i^2 - y_i^2]y_i + \omega_i x_i + G \sum_{j=1}^N C_{ij} (y_j - y_i) + \beta \eta_i(t) \quad (2)$$

Equations 1 and 2 describe the coupling of Stuart-Landau oscillators through an effective connectivity matrix C . The $x_i(t)$ term represents the simulated BOLD signal data of brain area i . The values of $y_i(t)$ are relevant to the dynamics of the system but are not part of the information read out from the system. In these equations, $\eta_i(t)$ provides additive Gaussian noise with standard deviation β . The Stuart-Landau oscillators for each brain area i express a Hopf normal form that has a supercritical bifurcation at $a_i=0$, so that if $a_i > 0$ the system has a stable limit cycle with frequency $f_i = \omega_i / 2\pi$ (where ω_i is the angular velocity); and when $a_i < 0$ the system has a stable fixed point representing a low activity noisy state. The intrinsic frequency f_i of each Stuart-Landau oscillator corresponding to a brain area is in the 0.008–0.08 Hz band ($i = 1, \dots, 360$). The intrinsic frequencies are fitted from the data, as given by the averaged peak frequency of the narrowband BOLD signals of each brain region. The coupling term representing the input received in node i from every other node j , is weighted by the corresponding effective connectivity C_{ij} . The coupling is the canonical diffusive coupling, which approximates the simplest (linear) part of a general coupling function. G denotes the global coupling weight, scaling equally the total input received in each brain area. While the oscillators are weakly coupled, the periodic orbit of the uncoupled oscillators is preserved. Details are provided in the [Supplementary Material](#).

The effective connectivity matrix is derived by optimizing the conductivity of each existing anatomical connection as specified by the Structural Connectivity matrix (measured with tractography [Huang et al. 2021]) in order to fit the empirical functional connectivity (FC) pairs and the lagged FC^{τ} pairs. By this, we are able to infer a non-symmetric Effective Connectivity matrix (see Gilson et al. 2016). Note that FC^{τ} , i.e. the lagged functional connectivity between pairs, lagged at τ s, breaks the symmetry and thus is fundamental for our purpose. Specifically, we compute the distance between the model FC simulated from the current estimate of the effective connectivity and the empirical data FC^{emp} , as well as the simulated model FC^{τ} and empirical data $FC^{\tau, \text{emp}}$ and adjust each effective connection (entry in the effective connectivity matrix) separately with a gradient-descent approach. The model is run repeatedly with the updated effective connectivity until the fit converges toward a stable value.

We start with the anatomical connectivity obtained with probabilistic tractography from dMRI (or from an initial zero C matrix as described in the [Supplementary Material](#)) and use the following procedure to update each entry C_{ij} in the effective connectivity matrix

$$C_{ij} = C_{ij} + \varepsilon \left((FC_{ij}^{\text{emp}} - FC_{ij}) + (FC_{ij}^{\tau, \text{emp}} - FC_{ij}^{\tau}) \right) \quad (3)$$

where ε is a learning rate constant, and i and j are the nodes. When updating each connection if the initial matrix is a dMRI structural connection matrix (see [Supplementary Material](#)), the corresponding link to the same brain regions in the opposite hemisphere is also updated, as contralateral connections are not revealed well

by dMRI. The convergence of the algorithm is illustrated by Rolls et al. (2022b), and the utility of the algorithm was validated as described in the [Supplementary Material](#).

For the implementation, we set τ to be 2 s (the shortest time in which with fMRI a $FC^{\tau, \text{emp}}$ different from FC^{emp} might be expected) selecting the appropriate number of TRs to achieve this. The maximum effective connectivity was set to a value of 0.2. The directionality of the effective connectivity measured here with fMRI with its necessary delay of $\tau = 2$ s was set to be consistent with projections forward up through sensory cortical hierarchies as confirmed with magnetoencephalography (Rolls et al. 2023f), and to be consistent with previous fMRI effective connectivity papers (Rolls et al. 2022a, 2022b, 2023a, 2023b, 2023d, 2023c, 2023e, 2023g, 2023h), as considered further in the [Supplementary Material](#).

Effective connectome

Whole-brain effective connectivity (EC) analysis was measured between the 19 frontal and related cortical regions described above (see [Figs. 1](#) and [S1](#)) and the 360 regions defined in the surface-based HCP-MMP atlas (Glasser et al. 2016a) in their reordered form provided in [Table S1](#), described in the [Supplementary material](#), and used in the volumetric extended HCPex atlas (Huang et al. 2022). This EC was computed for all 171 HCP participants for the whole resting state timeseries at 7T. The effective connectivity algorithm was run until it had reached the maximal value for the correspondence between the simulated and empirical functional connectivity matrices at time t and $t + \tau$ (see [Supplementary Material](#)). The effective connectivity calculated was checked and validated in a number of ways described in the [Supplementary Material](#) and elsewhere (Rolls et al. 2023b). The present algorithm was developed from an earlier approach that was extensively tested and validated (Gilson et al. 2016).

To test whether the vectors of effective connectivities of each of the 19 frontal and related cortex regions with the 180 areas in the left hemisphere of the modified HCP atlas were significantly different, the interaction term was calculated for each pair of the 19 frontal cortex regions effective connectivity vectors in separate two-way ANOVAs (each 2×180) across the 171 participants, and Bonferroni correction for multiple comparisons was applied. The results were checked with the non-parametric Scheirer-Rey-Hare test (Scheirer et al. 1976; Sinha 2022).

Functional connectivity

The functional connectivities ([Fig. 5](#)) which represent a linear measure of connectivity (calculated with the Pearson correlation) range from close to 1.0 to -0.33 and with a threshold of 0.4 reveal somewhat more links than the effective connectivity, partly perhaps because they can reflect common input to two regions rather than causal connectivity between regions, and partly because the threshold has been set to reveal effects known in the literature but not reflected in the effective connectivity. The functional connectivities are useful as a check on the effective connectivities, but of course do not measure directed “causal” effects.

For comparison with the effective connectivity, the functional connectivity was also measured at 7T with the identical set of 171 HCP participants, data, and filtering of 0.008–0.08 Hz. The functional connectivity was measured by the Pearson correlation between the BOLD signal timeseries for each pair of brain regions, and is in fact the FC^{emp} referred to above. A threshold of 0.4 is used for the presentation of the findings in [Fig. 5](#), for this sets the sparseness of what is shown to a level commensurate with the

effective connectivity, to facilitate comparison between the functional and the effective connectivity. The functional connectivity can provide evidence that may relate to interactions between brain regions, while providing no evidence about causal direction-specific effects. A high functional connectivity may in this scenario thus reflect strong physiological interactions between areas, and provides a different type of evidence to effective connectivity. The generative effective connectivity is non-linearly related to the functional connectivity, with effective connectivities being identified (i.e. greater than zero) only for the links with relatively high functional connectivity.

The functional connectivity is shown in Fig. 5 and the diffusion tractography in Fig. 6 for comparison with the effective connectivity. Functional connectivity and diffusion tractography have been used in many previous investigations of the human connectome (Catani and Thiebaut de Schotten 2008; Glasser et al. 2016a; Maier-Hein et al. 2017), and therefore the comparison with effective connectivity is of interest.

Connections shown with diffusion tractography

Diffusion tractography can provide evidence about fiber pathways linking different brain regions with a method that is completely different to the ways in which effective and functional connectivity are measured, so is included here to provide complementary and supporting evidence to the effective connectivity. Diffusion tractography shows only direct connections, so comparison with effective connectivity can help to suggest which effective connectivities may be mediated directly or indirectly. Diffusion tractography does not provide evidence about the direction of connections. Diffusion tractography was performed on 171 HCP participants imaged at 7T with methods described in detail elsewhere (Huang et al. 2021). The major parameters were: 1.05 mm isotropic voxels; a two-shell acquisition scheme with b-values=1,000, 2,000 s/mm², repetition time/echo time = 7,000/71 ms, 65 unique diffusion gradient directions and 6 b0 images obtained for each phase encoding direction pair (AP and PA pairs). Preprocessing steps included distortion correction, eddy-current correction, motion correction, and gradient non-linearity correction. In brief, whole brain tractography was reconstructed for each subject in native space. To improve the tractography termination accuracy in GM, MRtrix3's 5ttgen command was used to generate multi-tissue segment images (5tt) using T1 images, the segmented tissues were then co-registered with the b0 image in diffusion space. For multi-shell data, tissue response functions in GM, WM, and CSF were estimated by the MRtrix3' dwi2response function with the Dhollander algorithm (Dhollander et al. 2016). A Multi-Shell Multi-Tissue Constrained Spherical Deconvolution (MSMT-CSD) model with lmax=8 and prior co-registered 5tt image was used on the preprocessed multi-shell DWI data to obtain the fiber orientation distribution (FOD) function (Smith 2002; Jeurissen et al. 2014). Based on the voxel-wise fiber orientation distribution, anatomically constrained tractography (ACT) using the probabilistic tracking algorithm: iFOD2 (2nd order integration based on FOD) with dynamic seeding was applied to generate the initial tractogram (1 million streamlines with maximum tract length=250 mm and minimal tract length=5 mm). To quantify the number of streamlines connecting pairs of regions, the updated version of the spherical-deconvolution informed filtering of the tractograms (SIFT2) method was applied, which provides more biologically meaningful estimates of structural connection density (Smith et al. 2015).

The results for the tractography are shown in Fig. 6 as the number of streamlines between areas with a threshold applied of

10 to reduce the risk of occasional noise-related observations. The highest level in the color bar was set to 500 streamlines between a pair of cortical regions in order to show graded values for a number of links, but the value for the number of streamlines between V1 and V2 was in fact higher at close to 10,000. The term "connections" is used when referring to what is shown with diffusion tractography, and connectivity when referring to effective or functional connectivity.

The diffusion tractography (Fig. 6) provides no evidence on the direction or causality of connections, and is useful as it can provide some evidence on what in the effective connectivity may reflect a direct connection, and what does not. However, limitations of the diffusion tractography are that it cannot follow streamlines within the gray matter where the fibers become unmyelinated so the exact site of termination is not perfectly provided; and the tractography does not follow long connections well with for example almost none of the contralateral connectivity shown with tractography that is revealed by the effective connectivity in Figs. S2 and S3; and may thus overemphasize connections between close cortical regions. Nevertheless the diffusion tractography is a useful complement to the effective connectivity, especially where it provides evidence where an effective connectivity link may be mediated by a direct connection. On the other hand, the effective connectivity and functional connectivity are useful complements to the tractography by helping to exclude false positives in the tract-following in the tractography, as had been examined for the human hippocampal connectome (Huang et al. 2021; Ma et al. 2022; Rolls et al. 2022b).

Results

Overview: Effective connectivity, functional connectivity, and diffusion tractography

The effective connectivities to the six area 10 frontal pole and 13 other prefrontal cortex regions from other cortical regions in the left hemisphere are shown in Fig. 2. The effective connectivities from the 19 frontal cortical regions to other cortical regions in the left hemisphere are shown in Fig. 3. The vectors of effective connectivities of each of the 19 frontal cortical regions with the 180 regions in the left hemisphere of the HCP-MMP atlas were all significantly different from each other. (Across the 171 participants the interaction term in separate 2-way ANOVAs for the comparisons between the effective connectivity of every pair of the 19 regions of interest (ROIs) after Bonferroni correction for multiple comparisons were all $P < 10^{-90}$. The results were confirmed with the non-parametric Scheirer-Rey-Hare test (Scheirer et al. 1976; Sinha 2022) The text assumes reference to the data in Figs. 2–6. The effective connectivities described in the text are the stronger ones, typically > 0.01 where the maximum value is 0.2, but all of those greater than 0 are shown in the Figures. In addition to the effective connectivity, the functional connectivity (Fig. 5) and diffusion tractography (Fig. 6) available for each cortical region are referred to where useful. The functional implications of the results described next are considered in the Discussion, using Fig. 7 that provides a schematic diagram of the effective connectivity of frontal pole regions 10 pp, a10p, and p10p and which may be helpful to view when the Results are considered.

For convenience, and relating to the similarity of the connectivities of the different cortical regions analyzed, the regions are described in three main groups: Frontal Pole regions; Dorsal Prefrontal Cortex regions including i6–8 and s6–8; and Dorsolateral Prefrontal Cortex regions. The latter two groups of regions

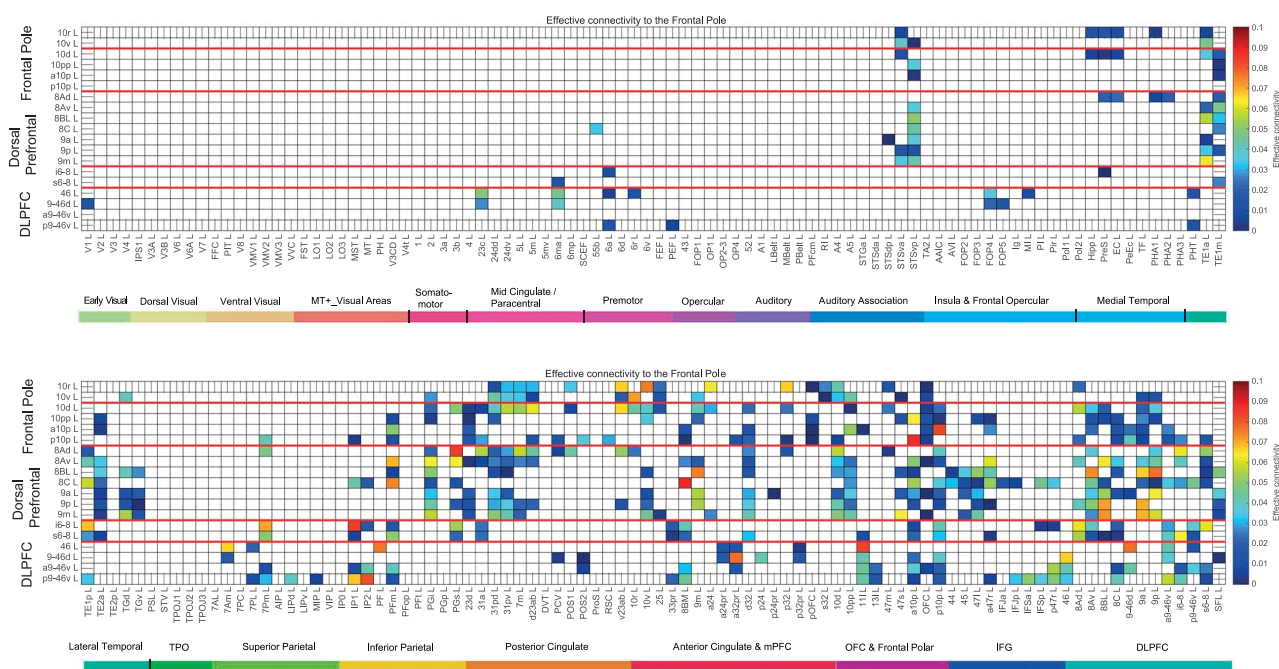


Fig. 2. Effective connectivity TO frontal cortical regions (the rows) FROM 180 cortical areas (the columns) in the left hemisphere. The effective connectivity is read from column to row. Effective connectivities of 0 are shown as blank. All effective connectivities found between this set of brain regions. The effective connectivity maps are scaled to show 0.15 as the maximum, as this is the highest effective connectivity found between this set of brain regions. The effective connectivity algorithm for the whole brain is set to have a maximum of 0.2, and this was for connectivity between V1 and V2. The effective connectivity for the first set of cortical regions is shown in the top panel; and for the second set of regions in the lower panel. Abbreviations: See Table S1. The six frontal pole regions of area 10 are above the second red line down; and for the second set of regions in the lower panel. Next are the dorsal prefrontal cortex regions, with the two transitional regions i6–8 and s6–8. Below the lower red line are regions of the HCP-MMP DLPFC division—Dorsolateral prefrontal cortex, which in the text are divided into dorsal prefrontal and dorsolateral prefrontal cortex groups. These regions are defined in the HCP-MMP atlas (Glasser et al. 2016a). The names of the cortical regions are as listed in the modified HCPex atlas Huang, Rolls et al. (2022), shown in Table S1.

are useful in this analysis by helping to elucidate what may be different about the connectivity of the frontal pole regions from other nearby and connected cortical systems.

Frontal Pole regions (10 pp, a10p, p10p, and 10d; and 10r and 10v) 10pp, a10p, p10p

10pp, a10p, p10p have somewhat similar connectivity to each other, and are considered together, with any differences clear in Figs. 2–6. These regions have some effective connectivity (Fig. 2) with the cortex in the superior temporal sulcus (STSva and STSvp); anterior inferior temporal cortex (TE1m, TE2a) which has semantic functions (Rolls et al. 2022a, 2023f); inferior parietal cortex (PFm and PGi, which are visual regions [Rolls et al. 2023d]); posterior cingulate division (especially d23ab, PCV, POS2, and RSC to p10p, which are implicated in memory by connecting “where” cortical regions with the hippocampus [Rolls et al. 2023h]); with some anterior cingulate/medial prefrontal cortex regions (10v and 8BM, 9m, a32pr, d32, p32) (Rolls et al. 2023c); from the orbitofrontal cortex (pOFC, 11l, and OFC; 47s, a47r [Rolls et al. 2023c]); with 47l closely associated with Broca’s area (Rolls et al. 2022a); with other frontal pole areas (a10p, p10p, 10pp); and with almost all Dorsal Prefrontal and DLPFC regions; but from no inferior prefrontal cortex regions.

Figure 3 shows that 10pp, a10p, and p10p considered together have effective connectivity directed to superior temporal sulcus STSvp; anterior inferior temporal TE1m and TE2a and temporal pole TGd; to inferior parietal cortex visual regions PFm, PGi, and PGs (Rolls et al. 2023d); to posterior cingulate division regions 23d,

31a, 31pd, 31pv, 7m, d23ab, PCV, POS2, and RSC; to anterior cingulate 8BM, 9m, a32pr, d32, p32; to orbitofrontal cortex pOFC, 13l, OFC, a47r, and p47r; to Broca’s 44, 45 and the closely associated 47l; and to almost all Dorsal and Dorsolateral Prefrontal cortex regions but almost no inferior prefrontal cortex regions.

Figure 4 shows that the effective connectivity of these three frontal pole regions measured with resting state fMRI is stronger from them to most other cortical regions with which they have effective connectivity. (This directionality of the effective connectivity was confirmed with that measured with fMRI in the HCP working memory task [Barch et al. 2013].)

The functional connectivity (Fig. 5) of these three frontal pole regions is generally consistent with the effective connectivity, with more functional connectivity with Dorsal and Dorsolateral prefrontal cortex (DLPFC) than inferior frontal gyrus (IF) regions.

The diffusion tractography (Fig. 6) shows some connections of these 3 frontal pole regions with the anterior insular cortex AAIC; the anterior cingulate cortex; the medial orbitofrontal cortex (pOFC, OFC, 13l and 11l); with the lateral orbitofrontal cortex (47s, 47l, a47r); with Broca’s 44, 45 and the closely related 47l (Rolls et al. 2022a); and with other prefrontal cortex regions especially 9-46d, 9-46v, and 9a.

10d

Region 10d receives effective connectivity (Fig. 2) from the cortex in the superior temporal sulcus (STSva); anterior inferior temporal cortex; inferior parietal cortex (PGi and PGs); the hippocampus, presubiculum, and entorhinal cortex; the posterior cingulate division (especially 23d, 31a, 31pd, 31pv, 7m, d23ab, and v23ab, the latter 4 of which are implicated in memory by connecting “what”

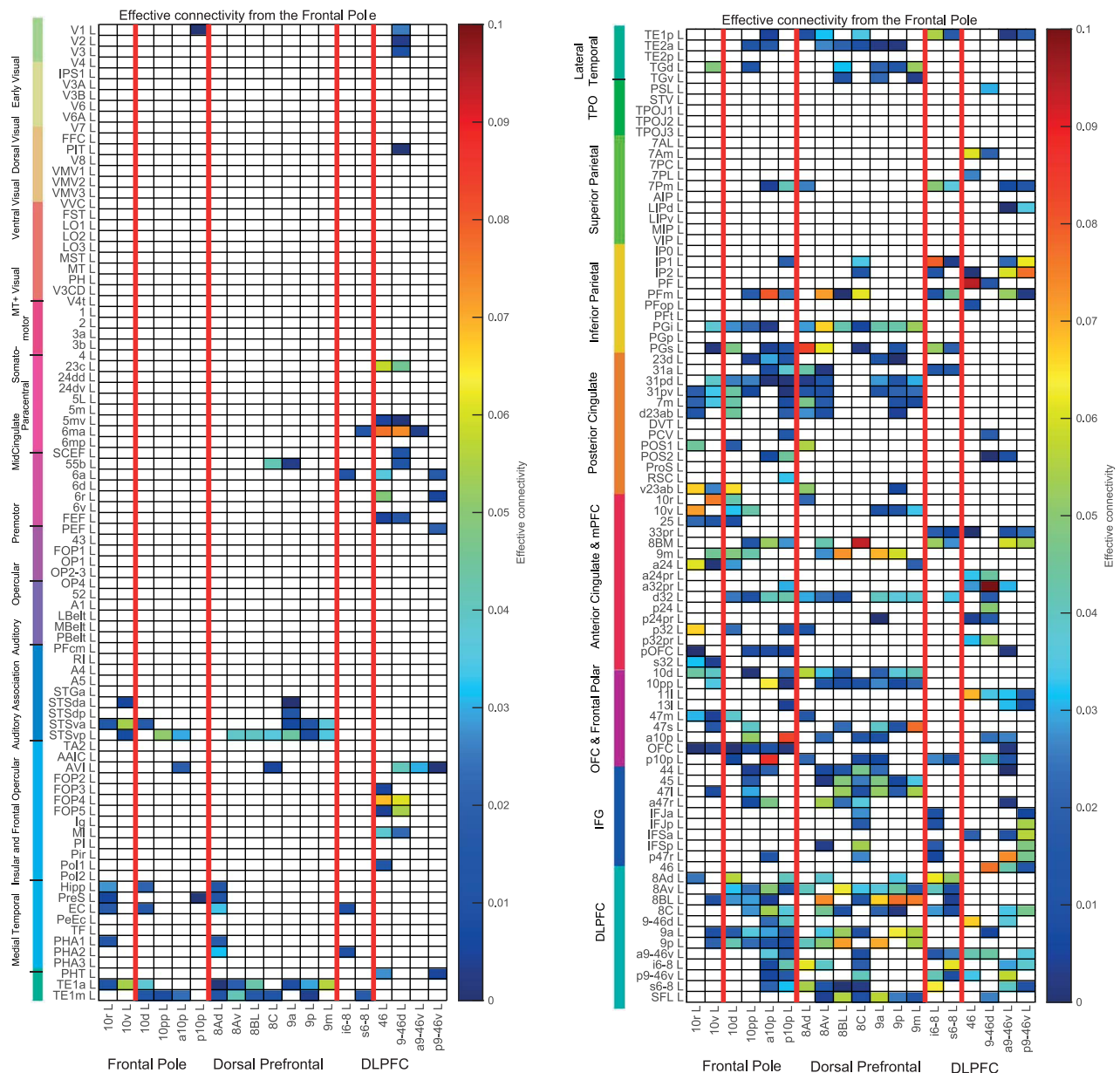


Fig. 3. Effective connectivity FROM the frontal cortical regions TO 180 cortical areas in the left hemisphere. The effective connectivity is read from column to row. Effective connectivities of 0 are shown as blank. Abbreviations: See Table S1. The divisions of frontal cortex areas are separated by red lines as in Fig. 2.

cortical regions with the hippocampus [Rolls et al. 2023h]); from 10r, 10v, and subgenual 25; from anterior cingulate 9m, a24, d32, p32; from the orbitofrontal cortex (OFC, 47m); from other frontal pole areas (p10p, 10pp); and from Dorsal Prefrontal regions (8Ad, 8Av, 8BL, 9a, and 9p).

Region 10d has connectivity toward (Fig. 3) the cortex in the superior temporal sulcus (STSva); anterior inferior temporal cortex; inferior parietal cortex (PGi and PGs); the hippocampus and entorhinal cortex; posterior cingulate division (especially 31pd, 31pv, 7m, d23ab, and v23ab, which are implicated in memory by connecting cortical regions with the hippocampus [Rolls et al. 2023h]); to 10r, 10v, and subgenual 25; to anterior cingulate 9m, a24, d32, and p32; to the orbitofrontal cortex (OFC, 47m); to another frontal pole area (p10p); and to Dorsal Prefrontal regions (8Ad, 8Av, 8BL, 9a, and 9p), but not to inferior frontal gyrus regions.

Figure 4 shows that the effective connectivity measured with fMRI is stronger from 10d to many of these cortical regions apart from the posterior cingulate regions and region OFC.

The functional connectivity for 10d (Fig. 5) is generally consistent (though of course provides no evidence about the directionality, as it is measured by correlations). The functional connectivity emphasizes greater connectivity of 10d with the Dorsal Prefrontal cortex than with the inferior frontal gyrus (IF regions).

The diffusion tractography for 10d (Fig. 6) indicates some connections with the insula (AAIC which may be visceral insula [Rolls et al. 2023e]), and the mid-insula (MI, which is somatosensory [Rolls et al. 2023e]); with 10r, 10v, and the nearby anterior cingulate cortex; with Broca's area 45 and with 47l both involved in language [Rolls et al. 2022a]; and with some Dorsal and Dorsolateral Prefrontal cortex regions.

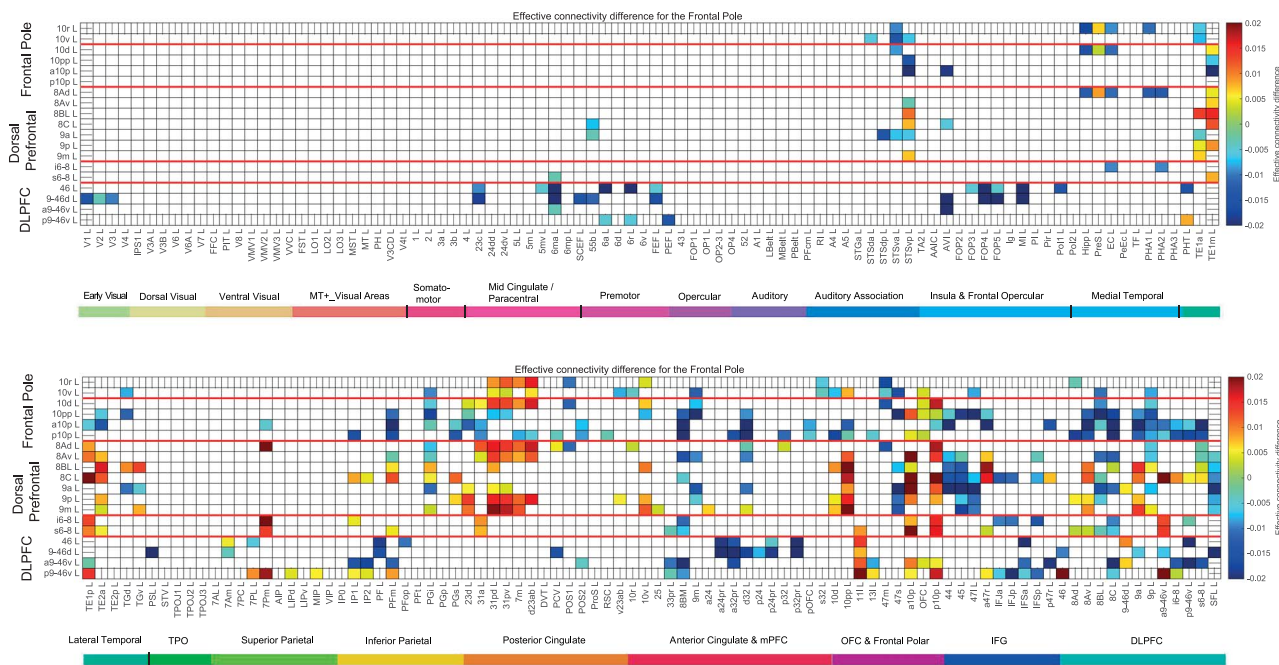


Fig. 4. Difference of the effective connectivity for frontal cortical regions with other cortical regions. For a given link, if the effective connectivity difference is positive, the connectivity is stronger in the direction from column to row. For a given link, if the effective connectivity difference is negative, the connectivity is weaker in the direction from column to row. This is calculated from 171 participants in the HCP imaged at 7T. The threshold value for any effective connectivity difference to be shown is 0.01. The abbreviations for the brain regions are shown in Table S1, and the brain regions are shown in Figs. 1 and S1. The effective connectivity difference for the first set of cortical regions is shown in the top panel; and for the second set of regions in the lower panel. Conventions as in Fig. 2.

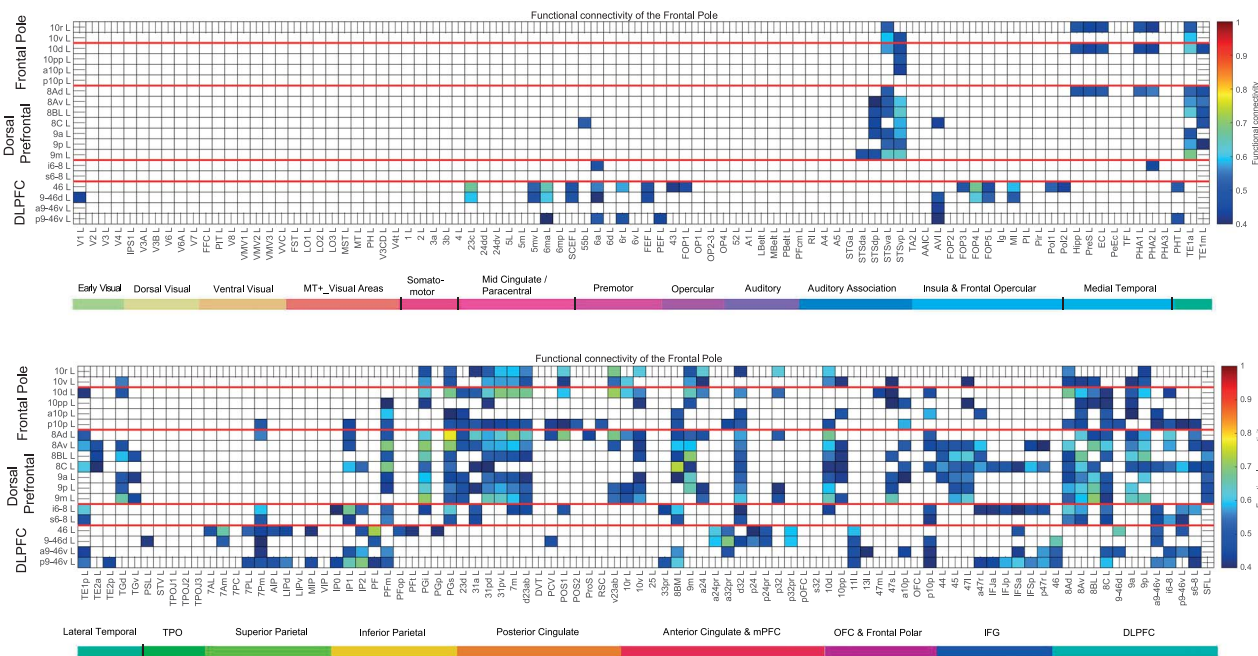


Fig. 5. Functional connectivity between frontal cortical regions and 180 other cortical regions in the left hemisphere. Functional connectivities < 0.4 are shown as blank. The upper figure shows the functional connectivity of the frontal cortical regions with the first half of the cortical regions; the lower figure shows the functional connectivity with the second half of the cortical regions. Abbreviations: See Table S1. Conventions as in Fig. 2.

10d differs from 10pp, a10p, and p10p in having more effective connectivity with the posterior cingulate cortex (Fig. 2) which is implicated in episodic memory (Rolls 2022, 2022b, 2023h).

10r and 10v

The effective connectivity of these regions as shown in Figs. 2 and 3 includes effective connectivity with the cortex in the

superior temporal sulcus (STS) (visual/semantic association [Rolls et al. 2022a, 2023b]); anterior inferior temporal cortex TE, and temporal pole TG, both multimodal semantic regions (Rolls et al. 2023f); hippocampus and entorhinal cortex; the posterior cingulate cortex (including 31pd, 31pv, d23ab, and v23ab) with are implicated in memory (Rolls et al. 2023h); anterior cingulate cortex (including especially pregenual areas a24, p24,

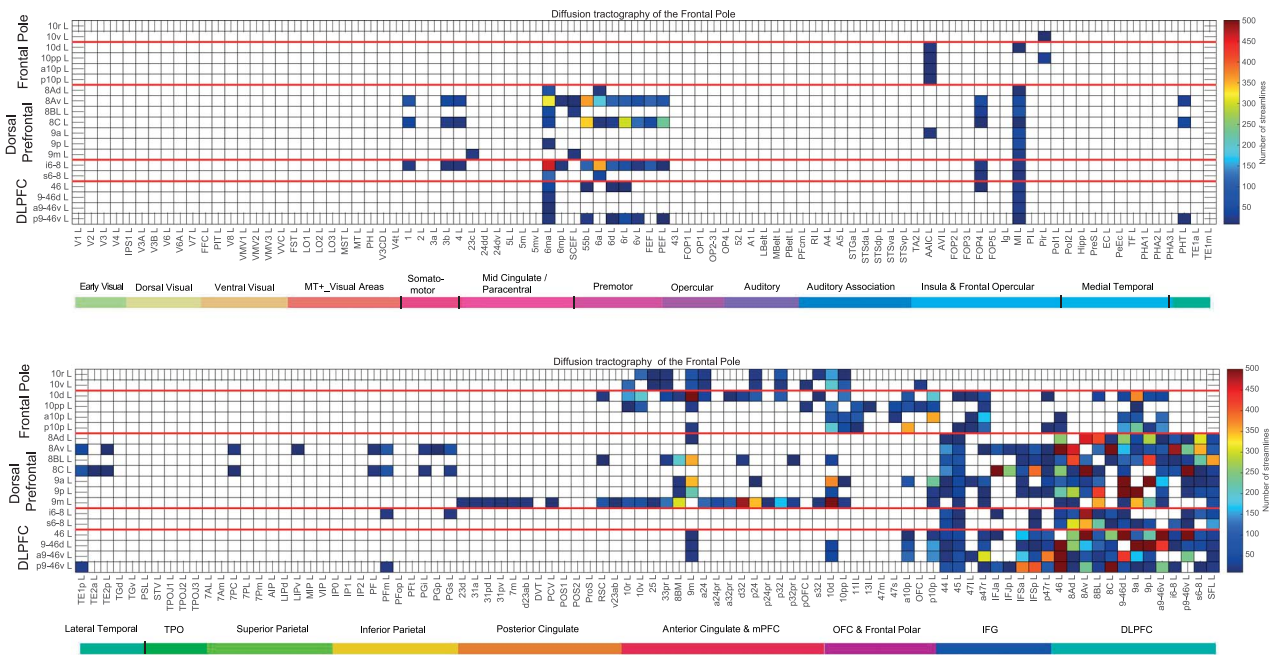


Fig. 6. Connections between the frontal cortical regions and 180 other cortical regions in the left hemisphere as shown by diffusion tractography using the same layout as in Figs. 2 and 4. The number of streamlines shown was thresholded at 10 and values less than this are shown as blank. The color bar was thresholded at 500 streamlines (see text). Abbreviations: See Table S1. Conventions as in Fig. 2.

and p32), and subgenual cingulate cortex area 25; and the medial orbitofrontal cortex (OFC) and lateral orbitofrontal cortex (47m and 47s).

For 10r and 10v, the directionality measured with task-related fMRI is stronger from rather than toward them apart from the posterior cingulate regions (Fig. 4). The diffusion tractography indicates direct connections of these area 10 regions with anterior cingulate cortex and the orbitofrontal cortex (pOFC and OFC) (Fig. 6).

10r and 10v have effective connectivity with frontal pole regions 10pp and p10p, and some effective connectivity with Dorsal Prefrontal regions (Figs. 2 and 3). Consistent with their more ventromedial and posterior location than other area 10 regions (Figs. 1 and S1-5), 10r and 10v have more connectivity with subgenual cingulate area 25, and with anterior cingulate s32 than other area 10 regions (Figs. 2 and 3).

Dorsal Prefrontal Cortex regions (8Ad, 8Av, 8BL, 8C, 9a, 9p, 9m; and intermediate regions i6–8 and s6–8)

In the dorsal part of the prefrontal cortex, **8Ad** has effective connectivity (Figs. 2 and 3) with anterior inferior temporal cortex (TE1a, TE1m); with visual inferior parietal regions PGs and PGI; with many anterior cingulate regions; and with frontal pole p10p, 10r, 10d, p10p. **8Ad** has substantial EC with other dorsal prefrontal regions 8Av, 9p, i6–8, and s6–8. **8Ad** has interesting EC with the episodic memory system, with entorhinal cortex EC, presubiculum and parahippocampal gyrus PHA1 and PHA2 (Rolls et al. 2022b; Rolls 2023c); and with “what” memory-related posterior cingulate cortex regions 31pd, 31pv, 7m, d23ab, and v23ab; and also with “where” posterior cingulate 31a, and POS1 (Rolls et al. 2023h). This connectivity may support functions of **8Ad** in visual and auditory top-down attention (Rolls et al. 2023e). With the resting state fMRI, the effective connectivities of **8Ad** show as stronger

from the inferior temporal and posterior cingulate cortices than in the reverse direction (Fig. 4).

8Av has somewhat similar connectivity to **8Ad**, though has stronger connectivity with anterior inferior temporal and inferior parietal visual regions including PFM (Figs. 2 and 3), so is likely to be involved mainly in visual processing, and its posterior cingulate connectivity is more related to the regions implicated in “what” memory-related processing. It has some effective connectivity with Broca’s regions 44, 45, and 471; and with orbitofrontal cortex a47r; and with frontal pole 10pp, a10p, and p10p. The effective connectivities of **8Av** show as stronger from the inferior temporal and posterior cingulate cortices than in the reverse direction (Fig. 4).

8BL located dorsally in the prefrontal cortex (Fig. 1) has similar connectivity to **8Av**, with especially pronounced effective connectivity with dorsally located prefrontal 9a and 9p (Figs. 2 and 3), and some connectivity with the temporal pole TGv and TGD.

8C has generally similar connectivities to **8BL**.

9a and **9p** have effective connectivity with superior temporal sulcus visual–auditory regions (STSdp, STSva, STSvp); with the hippocampus, and posterior cingulate division regions implicated in “what” episodic memory (31pd, 31pv, 23d [Rolls et al. 2023h]); with anterior inferior temporal semantic regions and the temporal pole; with inferior parietal visual regions PGI and PGs; with frontal pole regions (10v, 10d, 10pp, a10p, p10p); with anterior cingulate division regions 9m, d32, and orbitofrontal cortex 47s; with Broca’s area (44, 45, 471); and with dorsal frontal 8Av, 8Ad, 8BL, and 8C (Figs. 2 and 3). In contrast to dorsolateral prefrontal cortex regions, 9a and 9p have little effective connectivity with premotor cortex regions, with FOP4 and FOP5, with superior parietal and intraparietal regions, and with dorsolateral prefrontal cortex regions (Figs. 2 and 3). The connectivities of the anterior inferior temporal and posterior cingulate division regions are stronger with rsfMRI toward 9a and 9p than vice versa (Fig. 4). The functional connectivity is largely consistent (Fig. 5), and the

tractography provides evidence for direct connections with frontal pole regions 10d, 10pp, a10p, and p10p (Fig. 6).

9m is on the anterior medial wall of the prefrontal cortex (Fig. 1), and it is noted that it may be involved in effects of damage to or stimulation of the frontal pole, due to its location (Fig. 1). 9m has effective connectivity with superior temporal sulcus regions STSva and STSvp; with the anterior inferior temporal cortex TE1a and TE2a; with temporal pole TGd and TGv; with parietal PGi; with posterior cingulate division 23d, 31pd, 31pv; with 10v, 10d, and 10pp; with the anterior cingulate cortex a24, d32; with the lateral orbitofrontal cortex (47s); with Broca's area 45 and 47l; and with dorsal prefrontal cortex regions, especially 8Av, 8BL, 9a, and 9p. The effective connectivity of 9m is rather similar to that of frontal pole 10d, 10v, and 10r (Fig. S4), though with stronger effective connectivity with Dorsal Prefrontal regions 8Av, 9a, and 9p.

i6–8 and **s6–8** are transitional areas in the HCP-MMP atlas (Glasser et al. 2016a), and have effective connectivity to area 6 premotor cortex regions; with parietal 7PL, 7PM, and some intraparietal regions; visual inferior parietal PFm and PGs; some anterior cingulate regions; and with other Dorsal, Dorsolateral, and Inferior Prefrontal cortex regions (Figs. 2 and 3).

Dorsolateral Prefrontal Cortex regions (46, 9-46d, a9-46v, p9-46v)

Region **46** has effective connectivity (Figs. 2 and 3) with parietal area 7 regions; to somatosensory/motor regions including six, frontal opercular (FOP) and insular, and inferior parietal PF, PFop (Rolls et al. 2023e); with some dorsal (supracallosal) anterior cingulate regions (a24pr, a23pr, a32pr, p24pr, p32pr) implicated in action (Rolls et al. 2023c); and with some posterior cingulate division regions also linked to movements (Rolls et al. 2023h). Region 46 also has effective connectivity with medial orbitofrontal cortex 11l; and with other DLPFC regions 9-46d, a9-46v, and some other prefrontal cortex regions. The directionality of the connectivity (Fig. 4) measured with rs fMRI was more away from region 46 except for the medial orbitofrontal cortex 11l connectivity (Fig. 4). This connectivity links region 46 to working memory for body movement-related actions and planning.

9-46d, **a9-46v**, and **p9-46v** comprise the other main regions of the dorsolateral prefrontal cortex (Fig. 1, with 46), and have somewhat similar effective connectivities to each other (Figs. 2–4). They have connectivity with premotor cortex regions (6ma, 6a, 6r, 55b), and eye field regions FEF, PEF, and SCEF); with AVI, antero-ventral insula which is probably visceral; with frontal opercular regions FOP4 and FOP5 which are taste/higher order somatosensory (Rolls et al. 2023e); some connectivity with inferior temporal cortex TE regions; with anterior cingulate 8BM, 33pr, a24pr, a32pr, p24; with orbitofrontal cortex 11l, 13l, OFC; with inferior prefrontal cortex IFJa, IFJp, IFsa, IFsp; and with each other. Most of these dorsolateral prefrontal cortex regions also have connectivity with parietal cortex area 7 (e.g. 7PL, 7PM), and intraparietal regions (e.g. AIP, LIPd, MIP, IP1, and IP2), and visual inferior parietal PFm. These connectivities are consistent with functions of these regions in visual-spatial (“where”) working memory. The effective connectivity measured with rsfMRI is toward the dorsolateral prefrontal cortex from inferior temporal, parietal, and orbitofrontal cortex (consistent with these providing inputs to this short-term memory system); and from the dorsolateral prefrontal cortex regions to premotor areas such as area six regions and supracallosal anterior cingulate regions (consistent with these being outputs of this

short-term memory system [Rolls 2023a]) (Fig. 4). The functional connectivity emphasizes the connectivity of these dorsolateral prefrontal cortex regions with visual including many superior parietal cortex (area 7 and intraparietal) regions (Fig. 5), and the diffusion tractography provides evidence for direct connections with premotor regions (a key difference from frontal pole regions), with frontal pole regions (a10p, p10p); with insular and frontal opercular regions, and with Broca's area (44 and 45) (Fig. 6).

Effective connectivities of the 19 frontal and related regions with contralateral cortical regions

The effective connectivities of the 19 regions from contralateral cortical areas are shown in Fig. S2, and to contralateral cortical regions in Fig. S3. These connectivities illustrate the principle that each HCP-MMP cortical region tends to have the strongest effective connectivity contralaterally with the corresponding cortical region in the other hemisphere, and that this applies to frontal pole cortical regions as well as to other cortical regions. The fact that the Hopf effective connectivity algorithm shows this for each cortical region provides further evidence on the utility of the Hopf effective connectivity algorithm, because it identifies strong effective connectivity with a corresponding cortical region even though it is far away in the contralateral hemisphere.

Correlations between the connectivities of different cortical regions

Figure S4 shows the correlations between the effective connectivities of the regions described here. These correlation maps show that 10r, 10v, and 10d have relatively similar effective connectivities to each other; and that 10pp, a10p, and p10p have relatively similar effective connectivities to each other, with some correlation with 10d. The correlation matrices in Fig. S4 also provide evidence that the effective connectivities of the dorsolateral prefrontal regions (46, 9-46d, a9-46v, and p9-46v) tend to be correlated with each other. So do the connectivities of the dorsal prefrontal regions (8Ad, 8Av, 8BL, 9a, 9p, and 9m), with 8C an outlier correlated instead with some dorsolateral prefrontal cortex regions. Both these sets of prefrontal regions have connectivity with the frontal pole regions. In particular, 10r, 10v, and 10d have connectivities correlated with dorsal prefrontal cortex regions; and a10p and p10p with some Dorsal Prefrontal Cortex regions. The connectivities of frontal pole regions with the inferior prefrontal gyrus regions (IFJa, IFJp, IFSa, IFSp in Figs. 2 and 3) are less strong than with the Dorsolateral and Dorsal Prefrontal sets of regions.

Differences between the effective connectivity of the frontal pole, and dorsal and dorsolateral prefrontal cortex regions

Figures 2–4 show some of the ways in which the effective connectivity of the 6 frontal pole regions (10d, 10pp, a10p, p10p; and 10r and 10v) differs from that of the dorsal prefrontal and dorsolateral prefrontal cortex regions (DLPFC). The DLPFC regions have effective connectivity with some somatosensory/premotor regions (parts of area 5, 6, frontal opercular and insular regions and the eye fields FEF and PEF), and the frontal pole regions have much less. The same applies to connectivity with superior parietal and intraparietal regions. The same applies to the connectivity with inferior frontal gyrus (IF) regions.

The connectivity of the frontal pole regions with superior temporal sulcus regions is similar to that of dorsal prefrontal regions,

but DLPFC does not have this connectivity. It is mainly Dorsal Prefrontal and frontal pole regions that have connectivity with inferior temporal cortex and superior temporal sulcus regions, with much less connectivity of the DLPFC with the inferior temporal cortex and superior temporal sulcus regions.

An interesting and probably key feature of the frontal pole regions is that they have connectivity with medial orbitofrontal cortex regions pOFC, 11l and OFC, and anterior cingulate cortex regions.

Discussion

The aim of the Discussion is to draw out the implications for the organization and operation of frontal pole cortical regions from the effective connectivities complemented by the functional connectivity and diffusion tractography described here. The strengths of the effective connectivities are used as a guide, and so is evidence from neuronal recordings in comparable regions in macaques and neuroimaging activation studies in humans.

Frontal Pole regions (10d, 10pp, a10p, p10p; and 10r and 10v)

The key effective connectivities of the Frontal Pole regions are illustrated in Fig. 7. The Frontal Pole Regions have strong effective connectivity with Dorsal Prefrontal cortex, the Lateral Orbitofrontal cortex (area 47 regions) implicated in punishment and non-reward (Rolls et al. 2023a; Rolls 2023b), the Medial Orbitofrontal Cortex (especially OFC, pOFC, and 11l) involved in reward (Rolls et al. 2020, 2023a; Rolls 2023b), and the anterior cingulate regions (e.g. a24, p32, d32, and p32) implicated in reward (Rolls 2023b; Rolls et al. 2023c). The frontal pole also has effective connectivity with semantic/language-related regions (Rolls et al. 2022a) including the anterior temporal cortical TE regions, temporal pole (TG regions) and superior temporal sulcus (STS) regions; and visual inferior parietal cortex regions PFm, PGI, and PGs. There is also some connectivity with posterior cingulate cortex regions (e.g. 31pd and 31pv) implicated in memory (Rolls et al. 2023h).

One key difference of the effective connectivity of the frontal pole regions from the dorsolateral prefrontal cortex regions (46, 9-46d, a9-46v, p9-46v, and probably 8C given its connectivity shown in Figs. 2 and 3) is that the DLPFC regions have connectivity with area 6 premotor regions and the frontal pole regions do not. Another difference is that the frontal pole regions have connectivity with anterior temporal lobe TE, and superior temporal sulcus (STS) regions, whereas the DLPFC regions have connectivity with some parietal area 7 and intraparietal regions. These differences can be related to specialization of the DLPFC regions for working memory for spatial responses, with often visuo-spatial components (Rolls 2023a), whereas the frontal pole regions are more connected to semantic visual “what” representations. Another difference is that the frontal pole has more connectivity with both medial orbitofrontal cortex and anterior cingulate cortex regions implicated in reward (Rolls 2023b) and lateral orbitofrontal cortex regions implicated in non-reward than does the DLPFC (Figs. 2 and 3).

The dorsal prefrontal cortex regions (8AD, 8Av, 8BL, 9a, 9p, and 9m) share with the frontal pole regions connectivity with “what” temporal lobe representations (TE and STS regions). A key difference is that the frontal pole regions have much more effective connectivity with medial orbitofrontal cortex reward-related regions (11l, 13l, OFC, and pOFC) and anterior cingulate

cortex reward-related regions (e.g. a24, p32, s32) than do the dorsal prefrontal cortex regions. The frontal pole also has connectivity with the hippocampal system and posterior cingulate cortex, which allows interaction with memory-related processing (Rolls et al. 2023h).

Hypotheses about function based on these connectivities, especially for frontal pole regions a10p, p10p, and 10pp, arise as follows

The Dorsolateral Prefrontal cortex regions provide short-term or working memory for brain regions that include the premotor cortex, and visuo-spatial intraparietal and parietal area 7 regions, to provide working memory of visual-spatial including body responses (Funahashi et al. 1989; Goldman-Rakic 1996; Petrides and Pandya 1999; Goldman and Leung 2002; Passingham 2021) by maintaining firing in an attractor network (Martinez-Garcia et al. 2011; Fuster 2015; Constantinidis et al. 2018; Lundqvist et al. 2018; Rolls 2021b, 2023a). These dorsolateral prefrontal cortex regions are thereby involved in working memory and executive function (Baddeley 2012; Miller 2013; Miller et al. 2018; Baddeley et al. 2019; Baddeley 2021; Fuster 2021; Passingham 2021). For short-term memory to operate as expected, the connections should be strong to the short-term memory networks (in the DLPFC) so that new information that arrives can get into the short-term memory buffers, and weaker in the return direction so that the short term memory information does not dominate in the more posterior cortical regions that process incoming inputs from the world (Renart et al. 2001; Rolls 2016a, 2023a). Further, the DLPFC regions have outputs to premotor and related regions, so that when actions must be produced to remembered stimuli, or internally generated instead of being produced by inputs to sensory systems from the world, the DLPFC regions can lead to behavior from these internally maintained or generated representations (Rolls 2023a). The connectivities described here are consistent with and support these computational approaches to understanding brain function (Rolls 2023a).

The Dorsal Prefrontal regions with their connectivity with many semantic “what” systems described above may play an important role in top-down attention (Germann and Petrides 2020a, 2020b; Passingham 2021) by providing a working memory for “what” must be maintained as the subject of the attention (Deco and Rolls 2003, 2004, 2005a, 2005b). This functionality is likely to be important in executive function (Baddeley 2012; Miller 2013; Miller et al. 2018; Baddeley et al. 2019; Baddeley 2021; Fuster 2021; Passingham 2021).

Given that the DLPFC and Dorsal Prefrontal regions are involved in working memory and executive function, the computational issue then arises of for how long these working memory states should be maintained, or whether behavior should change, especially depending for example on how rewarding the current behavior is in relation to possible alternative behaviors. In this context, and given the connectivity of the frontal pole revealed in this investigation, the following new computational theory is proposed for the functioning of the frontal pole. It is proposed that the reward-related medial Orbitofrontal Cortex and pregenual anterior cingulate cortex (Rolls 2023b) and punishment and non-reward related Lateral Orbitofrontal Cortex (Rolls 2023b) provide information to the Frontal Pole regions about what rewards are being obtained and how rewarding they still are, and that this information from the Frontal Pole can then be used to reset the working memory attractor states in the Dorsolateral Prefrontal

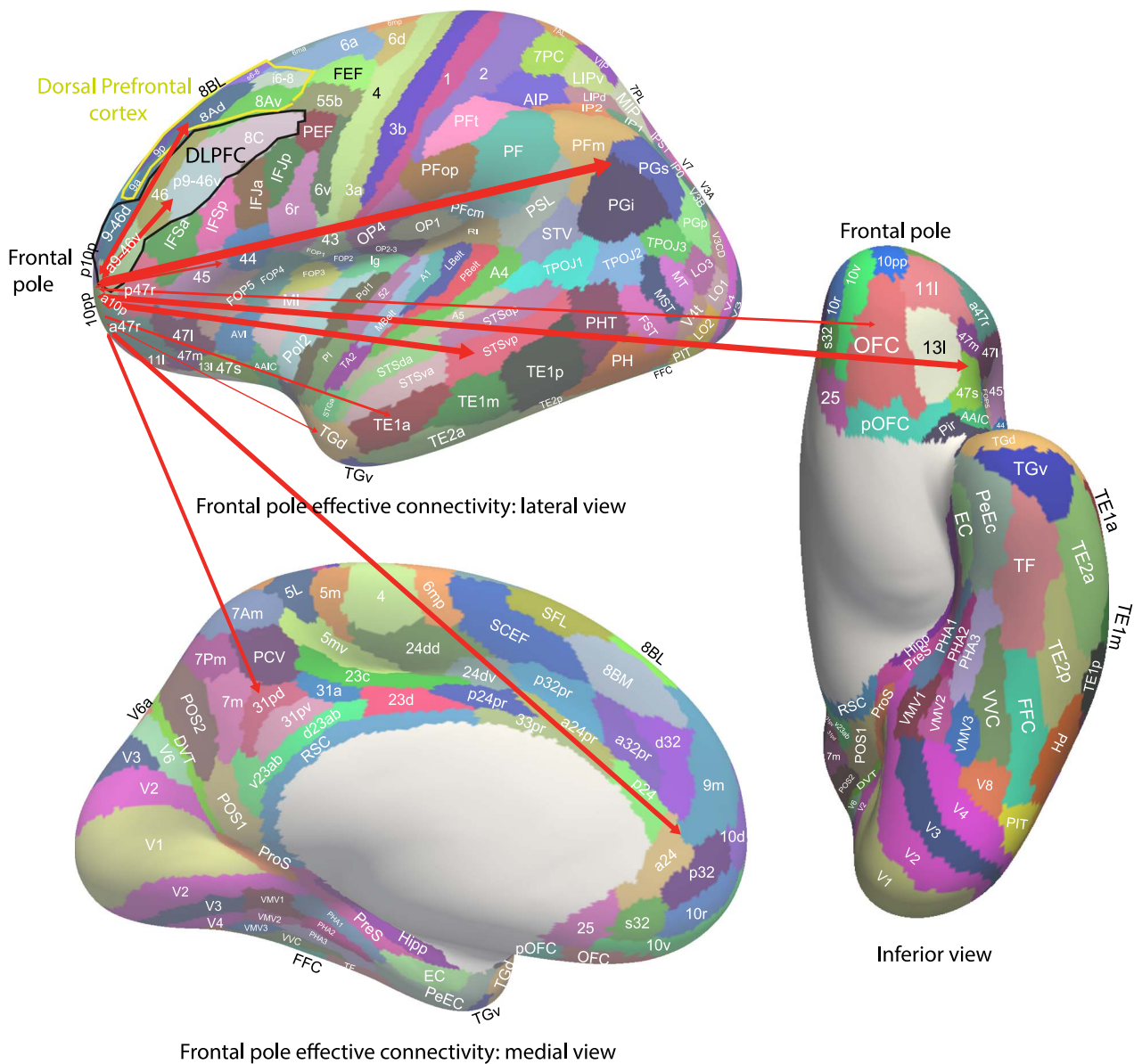


Fig. 7. Effective connectivity of the human frontal pole (especially a10p, p10p, 10 pp, and 10d): Schematic diagram. The width of the arrows reflects the effective connectivity with the size of the arrowheads reflecting the connectivity in each direction. The dorsolateral prefrontal cortex (DLPFC) regions are surrounded with a black line. The dorsal prefrontal cortex regions are surrounded by a yellow line. The frontal pole regions have strong effective connectivity with the DLPFC, dorsal prefrontal cortex, the lateral orbitofrontal cortex (area 47 regions) implicated in punishment and non-reward; and the medial orbitofrontal cortex (especially 11l but also 13l, OFC and pOFC) and anterior cingulate regions (e.g. a24, p32, and d32) involved in reward. The frontal pole also has effective connectivity with semantic/language-related regions including the anterior temporal cortical TE regions, temporal pole (TG regions) and superior temporal sulcus (STS) regions; visual inferior parietal cortex regions PFm, PGI, and PGI; and Broca's area 44 and 45. There is also some connectivity with posterior cingulate cortex regions (e.g. 31pd and 31pv) implicated in memory. The sulci have been opened sufficiently to show the cortical regions in the sulci. The cortical regions are defined in the human connectome project multi-modal Parcellation atlas (Glasser et al. 2016; Huang et al. 2022). The abbreviations are provided in Table S1.

and Dorsal Prefrontal cortex so that the behavior changes from the current plan or strategy that is normally maintained by the DLPFC and Dorsal Prefrontal Cortex working memory systems. In this way, it is now proposed, the reward and punishment signals from the Orbitofrontal Cortex can control, based on the amount of reward currently being received, whether the current behavior should be maintained in what can be considered as exploitation as reward is being received, or whether the behavior should change to what can be considered as exploration, given that smaller rewards, and/or non-reward, is now being received.

A key component in this exploit versus explore functionality for foraging mediated by the orbitofrontal and anterior cingulate cortex via the Frontal Pole could it is now proposed be sensory-specific satiety, the property computed in the orbitofrontal cortex of a gradual reduction in the reward value of a particular sensory stimulus being received over several minutes, without reduction in the reward value of other stimuli (Rolls et al. 1986, 1989; Critchley and Rolls 1996; Rolls 2016b, 2023a, 2023b). Sensory-specific satiety is computed in the orbitofrontal cortex (Rolls et al. 1989; Critchley and Rolls 1996; Kringelbach et al. 2003; Rolls 2023b).

In addition, the connectivity of the frontal pole regions not only with (mainly to, Fig. 4) DLPFC and Dorsal Prefrontal systems, but also to the STS, anterior inferior temporal cortex, and inferior parietal cortex, etc. (Figs. 4 and 7), provides evidence that the frontal pole cortex can influence the states in all of these brain regions. Assuming that the Frontal Pole cortex implements autoassociation networks with attractor dynamics (which is the general rule of operation provided in the neocortex by the recurrent collaterals between nearby pyramidal cells [Rolls 2016a, 2021b, 2021a, 2023a]), the implication is that the Frontal Pole can control the stability of all of these other cortical systems to which it has effective connectivity. In particular, if the frontal pole regions are in a deep and stable attractor, then this will tend to maintain other high-level cortical regions stable, so that behavior will continue, without change, to focus on the current task. However, if the frontal pole attractors do receive input from the medial orbitofrontal and anterior cingulate cortex encoding outcome value and expected value, and the lateral orbitofrontal encoding non-reward and punishment (Grabenhorst and Rolls 2011; Rolls 2019, 2023a, 2023b), then the frontal pole attractor may be knocked out of its stable state, which removes the top-down stabilizing effect on these other brain regions, and so behavior will switch to explore other perhaps more attractive or less punishing alternatives. It is proposed here for the first time that this is the basis for the exploit versus explore competition that controls behavior (Averbeck 2015; Mansouri et al. 2017a; Mansouri et al. 2017b; Hogeveen et al. 2022a; Hogeveen et al. 2022b). If the frontal pole cortex dynamics is highly stable, then behavior will continue to focus on the current task. If the frontal pole gets knocked out of its attractor by an incoming input, such as reward, non-reward, or punishment, then behavior will change, to explore alternatives. The frontal pole may in this way, lying at the top of the frontal lobe system, control not only the prefrontal cortex working memory regions in the Dorsal Prefrontal Cortex and DLPFC, but may also directly influence anterior temporal and STS, and inferior parietal areas (Rolls et al. 2023a).

The other area 10 regions, 10r, 10v, 10d, which continue into the ventromedial prefrontal cortex (Figs. 1 and S1-5), do have effective connectivity with the 3 frontal pole regions a10p, p10p, and 10pp, but also have connectivity with reward-related medial orbitofrontal cortex (OFC, pOFC) and pregenual anterior cingulate cortex regions (a24, d32, p32, s32); and with punishment/non-reward lateral orbitofrontal cortex regions (47m, 47s) (Figs. 2-4). In the theory, this reward/punishment-related information (Rolls 2023b) may be part of what can destabilize the frontal pole attractors when an especially large reward or non-reward or punishment is received. In this way, they may contribute to the explore part of the exploit versus explore frontal pole mechanisms. These ventromedial prefrontal and related area 10 regions are also notable in having connectivity with the memory-related posterior cingulate cortex (Figs. 2-4; [Rolls et al. 2023h]), which also receives inputs from the orbitofrontal cortex/anterior cingulate cortex reward/punishment/non-reward system (Rolls 2022; Rolls et al. 2023c, 2023h).

This is then the outline of a computational theory of how the Frontal Pole regions are involved in the behavioral strategies of "exploit vs explore".

In macaques the connections and neuronal recordings suggest the following subregions of the dorsolateral prefrontal cortex (Petrides and Pandya 1999; Kelly et al. 2010; Petrides et al. 2012; Yeterian et al. 2012; Petrides 2014; Pandya et al. 2015; Goulas et al. 2017; Passingham 2021). The posterior part near the arcuate sulcus contains a frontal eye field FEF. A dorsal part, FEFd is closely

associated with the immediately anterior 8Ad (part of the human Dorsal Prefrontal system described here) which has connectivity with dorsal stream intraparietal regions, and a ventral part FEFv is closely associated with the immediately anterior 8Av which has connectivity with ventral stream inferior temporal visual cortex regions (Petrides and Pandya 1999; Passingham 2021). The FEF and the adjacent area 46 cortex in the posterior part of the principal sulcus is especially implicated in eye movements to visual stimuli remembered over a short delay (Funahashi et al. 1989, 1993; Goldman-Rakic 1996), consistent with short-term memory functions of the dorsal prefrontal regions. The more mid and anterior parts of area 46 in the macaque principal sulcus correspond more to the human DLPFC regions described here and are involved more in remembered limb movements (Passingham 2021). In humans, area 46 is far anterior (Sallet et al. 2013), and probably includes some of 46 and a9-46v in the HCP-MMP atlas (Glasser et al. 2016a; Huang et al. 2022) (Fig. 1).

The use of effective connectivity

Effective connectivity is helpful in enabling estimation of the connectivity in each direction between every pair of brain regions, and is consistent with causal effects. Effective connectivity thus helps us to build hypotheses about how information flows through the system, and that is helpful, when complemented with evidence about what is represented in each brain region and the effects of damage to each brain region, in building a model of how the brain works computationally (Rolls 2021a, 2023a). This helps in understanding the serial nature of information processing in some of the sensory cortical hierarchies (Rolls 2021a), including the somatosensory cortical hierarchy described here that reaches inferior parietal PF. However, at the same time the effective connectivity makes it clear that in most cases there is at least some connectivity in the opposite direction, and the utility of this for processes such as memory recall, and top-down attention, is starting to be understood computationally (Treves and Rolls 1994; Deco and Rolls 2005a; Rolls 2016a, 2018, 2021a, 2022, 2023a). It must also be understood that there is considerable selectivity of the connectivity, with the mean sparseness of the connectivity 0.11 (meaning that on average any one cortical region makes connections with only ~11% of other cortical regions, with the selectivity greater than this when it is recognized that the number of strong connectivities is much smaller than this) in this series of papers (Rolls et al. 2022a, 2022b, 2023b, 2023d, 2023c, 2023e, 2023g, 2023h). The implication of this is that different sensory cortical systems can operate relatively independently of each other in their early stages of the hierarchy, and can then be brought together with signals from other hierarchies after several stages to form multimodal representations that lead eventually to semantic representations (Rolls 2021a; Rolls et al. 2022a, 2023b).

Conclusions

It is shown in this paper that the frontal pole regions have connectivity with reward-related systems in the orbitofrontal and anterior cingulate cortex, and also connectivity directed toward the dorsal prefrontal and dorsolateral prefrontal cortices involved in working memory and executive function, the anterior temporal lobe, and the inferior parietal cortex. Taking into account also the evidence implicating the frontal pole in exploit versus explore (Hogeveen et al. 2022a, 2022b), the theory is advanced that the reward value inputs to the frontal pole cortex are involved in controlling the stability of the networks in the dorsal and dorsolateral prefrontal, anterior temporal, and inferior parietal cortical areas

to influence whether to maintain behavior in exploit mode, or to change behavior in explore mode. In more detail, the frontal pole regions, especially a10p, p10p, and 10 pp, may, lying at the top of the frontal lobe system, control the dorsolateral prefrontal cortex (DLPFC) and Dorsal Prefrontal Cortex regions each of which has its own particular short-term memory to implement for a parietal or temporal lobe cortical sensory system. The control exerted by these frontal pole regions is proposed to be of whether to continue with the current task (exploitation), or whether to change behavior to explore other possible strategies, goals, or tasks. The frontal pole attractors, if stable, may maintain exploitation. But if an input from for example the orbitofrontal cortex or anterior cingulate cortex indicates better expected value, or non-reward or punishment, then the frontal pole autoassociation networks may be knocked out of their attractor, and without that stabilizing effect on the DLPFC and Dorsal Prefrontal and temporal and parietal systems, behavior may change to “explore”. The frontal pole may thus play an important role in implementing efficient strategies to perform tasks perhaps with competing goals and demands, by influencing whether to stay focussed and exploit, or to shift to explore whether another goal or strategy is more rewarding. The frontal pole cortex may provide a single computational system that receives value inputs from the orbitofrontal cortex and resets if the reward value has adapted or has become too low, and that can then control with a single output the stability of the other specialized working memory regions in the DLPFC and Dorsal prefrontal cortex. This single controller in the frontal pole is likely to be more efficient than having the reward value system attempt to contact directly every brain system that needs to be reset, with the possibility that some but not others would change state at any one time.

The other area 10 regions, 10v, 10r, and 10d, extend more posteriorly and ventrally into the ventromedial prefrontal cortex (Fig. 7), receive connectivity from the orbitofrontal cortex (Rolls et al. 2023c), and due to their connectivity with a10p, p10p, and 10pp help to introduce into that frontal pole circuitry reward, punishment and non-reward signals (Grabenhorst and Rolls 2011; Rolls 2023a, 2023b) that among others might produce a shift from exploit to explore. Indeed, a key finding here is the effective connectivity between the orbitofrontal cortex and frontal pole cortex, which provides a route to the frontal pole for rewards to be monitored, so that behavior can change when rewards change.

The Dorsal Prefrontal cortex regions in contrast have their particular short-term memory to implement for temporal lobe and parietal cortical system mainly involved in semantic representations, i.e. about “what” should be remembered. These dorsal prefrontal regions that include 8Ad and 8Av have connectivity with visual/semantic regions of the inferior parietal cortex including PGs and PGi, and also with the hippocampal system and memory-related parts of the posterior cingulate cortex, and are implicated in visual attention which requires a short-term memory to maintain the top-down bias for biased competition (Deco and Rolls 2005a; Deco and Rolls 2005b; Rolls 2021a, 2023a).

The dorsolateral prefrontal cortex (DLPFC) regions that include area 46 have connectivity from parietal area 7 and intraparietal regions and connectivity to premotor cortex regions, and are implicated in working memory for actions including body and visuomotor actions such as reaching and grasping, and in humans provide the basis for linked steps of plans with each step held in working memory (Rolls 2023a).

Acknowledgments

The neuroimaging data were provided by the Human Connectome Project, WU-Minn Consortium (Principal Investigators: David Van Essen and Kamil Ugurbil; 1U54MH091657) funded by the 16 NIH Institutes and Centers that support the NIH Blueprint for Neuroscience Research; and by the McDonnell Center for Systems Neuroscience at Washington University. Dr Wei Cheng and Shitong Xiang of ISTBI, Fudan University, Shanghai are thanked for parcellating the data into HCP-MMP surface-based space (Glasser et al. 2016a) and reordering it into HCPex order (Huang et al. 2022). Roscoe Hunter of the University of Warwick is thanked for contributing to the description in the [Supplementary Material](#) of the Hopf effective connectivity algorithm.

Ethical permissions

No data were collected as part of the research described here. The data were from the Human Connectome Project, and the WU-Minn HCP Consortium obtained full informed consent from all participants, and research procedures and ethical guidelines were followed in accordance with the Institutional Review Boards (IRB), with details at the HCP website <http://www.humanconnectome.org/>.

Author contributions

Edmund Rolls designed and performed the research, and wrote the paper. Gustavo Deco provided the effective connectivity algorithm. Chu-Chung Huang performed the diffusion tractography and prepared the coronal brain figures with the HCP-MMP labels in the Supplementary material. Jianfeng Feng performed the funding acquisition. All authors approved the paper. Edmund Rolls (Conceptualization, Data curation, Formal analysis, Investigation, Methodology, Project administration, Resources, Software, Supervision, Validation, Visualization, Writing—original draft, Writing—review & editing), Gustavo Deco (Formal analysis, Investigation, Methodology, Writing—review & editing), Chu-Chung Huang (Formal analysis, Investigation, Methodology, Writing—review & editing), and Jianfeng Feng (Funding acquisition, Writing—review & editing)

Supplementary material

[Supplementary material](#) is available at *Cerebral Cortex* online.

Funding

The work was supported by the following grants. Professor J. Feng: National Key R&D Program of China (No. 2019YFA0709502); 111 Project (No. B18015); Shanghai Municipal Science and Technology Major Project (No. 2018SHZDZX01), ZJLab, and Shanghai Center for Brain Science and Brain-Inspired Technology; and National Key R&D Program of China (No. 2018YFC1312904). G.D. is supported by a Spanish national research project (ref. PID2019-105772GB-I00 MCIU AEI) funded by the Spanish Ministry of Science, Innovation and Universities (MCIU), State Research Agency (AEI); HBP SGA3 Human Brain Project Specific Grant Agreement 3 (grant agreement no. 945539), funded by the EU H2020 FET Flagship program; SGR Research Support Group support (ref. 2017 SGR 1545), funded by the Catalan Agency for Management of University and Research Grants (AGAUR); Neurotwin Digital twins for model-driven non-invasive electrical brain stimulation (grant agreement ID: 101017716) funded by the EU H2020 FET Proactive program; euSNN European School of Network Neuroscience

(grant agreement ID: 860563) funded by the EU H2020 MSCA-ITN Innovative Training Networks; CECH The Emerging Human Brain Cluster (Id. 001-P-001682) within the framework of the European Research Development Fund Operational Program of Catalonia 2014–2020; Brain-Connects: Brain Connectivity during Stroke Recovery and Rehabilitation (id. 201725.33) funded by the Fundacio La Marato TV3; Corticity, FLAG-ERA JTC 2017, (ref. PCI2018-092891) funded by the Spanish Ministry of Science, Innovation and Universities (MCIU), State Research Agency (AEI). The funding sources had no role in the study design; in the collection, analysis and interpretation of data; in the writing of the report; and in the decision to submit the article for publication.

Conflict of interest statement: The authors have no competing interests to declare.

Data and code availability

The data are available at the HCP website <http://www.humanconnectome.org/>. Code for the Hopf effective connectivity algorithm is available at <https://github.com/decolab/Effective-Connectivity-Hopf>.

References

- Averbeck BB. Theory of choice in bandit, information sampling and foraging tasks. *PLoS Comput Biol*. 2015;11(3):e1004164.
- Baddeley A. Working memory: theories, models, and controversies. *Annu Rev Psychol*. 2012;63(1):1–29.
- Baddeley AD. Developing the concept of working memory: the role of neuropsychology. *Arch Clin Neuropsychol*. 2021;36:861–873.
- Baddeley AD, Hitch GJ, Allen RJ. From short-term store to multicomponent working memory: the role of the modal model. *Mem Cogn*. 2019;47(4):575–588.
- Bajaj S, Adhikari BM, Friston KJ, Dhamala M. Bridging the gap: dynamic causal Modeling and granger causality analysis of resting state functional magnetic resonance imaging. *Brain Connect*. 2016;6(8):652–661.
- Baker CM, Burks JD, Briggs RG, Conner AK, Glenn CA, Morgan JP, Stafford J, Sali G, McCoy TM, Battiste JD, et al. A Connectomic atlas of the human cerebrum-chapter 2: the lateral frontal lobe. *Oper Neurosurg (Hagerstown)*. 2018a;15(suppl_1):S10–S74.
- Baker CM, Burks JD, Briggs RG, Conner AK, Glenn CA, Robbins JM, Sheets JR, Sali G, McCoy TM, Battiste JD, et al. A Connectomic atlas of the human cerebrum-chapter 5: the insula and Opercular cortex. *Oper Neurosurg (Hagerstown)*. 2018b;15(suppl_1):S175–S244.
- Baker CM, Burks JD, Briggs RG, Conner AK, Glenn CA, Taylor KN, Sali G, McCoy TM, Battiste JD, O'Donoghue DL, et al. A Connectomic atlas of the human cerebrum-chapter 7: the lateral parietal lobe. *Oper Neurosurg (Hagerstown)*. 2018c;15(suppl_1):S295–S349.
- Baker CM, Burks JD, Briggs RG, Milton CK, Conner AK, Glenn CA, Sali G, McCoy TM, Battiste JD, O'Donoghue DL, et al. A Connectomic atlas of the human cerebrum-chapter 6: the temporal lobe. *Oper Neurosurg (Hagerstown)*. 2018d;15(suppl_1):S245–S294.
- Baker CM, Burks JD, Briggs RG, Sheets JR, Conner AK, Glenn CA, Sali G, McCoy TM, Battiste JD, O'Donoghue DL, et al. A Connectomic atlas of the human cerebrum-chapter 3: the motor, premotor, and sensory cortices. *Oper Neurosurg (Hagerstown)*. 2018e;15(suppl_1):S75–S121.
- Barbas H. General cortical and special prefrontal connections: principles from structure to function. *Annu Rev Neurosci*. 2015;38(1):269–289.
- Barch DM, Burgess GC, Harms MP, Petersen SE, Schlaggar BL, Corbetta M, Glasser MF, Curtiss S, Dixit S, Feldt C, et al. Function in the human connectome: task-fMRI and individual differences in behavior. *NeuroImage*. 2013;80:169–189.
- Catani M, Thiebaut de Schotten M. A diffusion tensor imaging tractography atlas for virtual in vivo dissections. *Cortex*. 2008;44(8):1105–1132.
- Catani M, Dell'acqua F, Vergani F, Malik F, Hodge H, Roy P, Valabregue R, Thiebaut de Schotten M. Short frontal lobe connections of the human brain. *Cortex*. 2012;48(2):273–291.
- Colclough GL, Smith SM, Nichols TE, Winkler AM, Sotiropoulos SN, Glasser MF, Van Essen DC, Woolrich MW. The heritability of multi-modal connectivity in human brain activity. *elife*. 2017;6:e20178.
- Constantinidis C, Funahashi S, Lee D, Murray JD, Qi XL, Wang M, Arnsten AFT. Persistent spiking activity underlies working memory. *J Neurosci*. 2018;38(32):7020–7028.
- Critchley HD, Rolls ET. Hunger and satiety modify the responses of olfactory and visual neurons in the primate orbitofrontal cortex. *J Neurophysiol*. 1996;75(4):1673–1686.
- Deco G, Rolls ET. Attention and working memory: a dynamical model of neuronal activity in the prefrontal cortex. *Eur J Neurosci*. 2003;18(8):2374–2390.
- Deco G, Rolls ET. A neurodynamical cortical model of visual attention and invariant object recognition. *Vis Res*. 2004;44(6):621–642.
- Deco G, Rolls ET. Attention, short-term memory, and action selection: a unifying theory. *Prog Neurobiol*. 2005a;76(4):236–256.
- Deco G, Rolls ET. Neurodynamics of biased competition and cooperation for attention: a model with spiking neurons. *J Neurophysiol*. 2005b;94(1):295–313.
- Deco G, Cabral J, Woolrich MW, Stevner ABA, van Hartevelt TJ, Kringelbach ML. Single or multiple frequency generators in ongoing brain activity: a mechanistic whole-brain model of empirical MEG data. *NeuroImage*. 2017a;152:538–550.
- Deco G, Kringelbach ML, Jirsa VK, Ritter P. The dynamics of resting fluctuations in the brain: metastability and its dynamical cortical core. *Sci Rep*. 2017b;7(1):3095.
- Deco G, Cruzat J, Cabral J, Tagliazucchi E, Laufs H, Logothetis NK, Kringelbach ML. Awakening: predicting external stimulation to force transitions between different brain states. *Proc Natl Acad Sci*. 2019;116(36):18088–18097.
- Dhollander T, Raffelt D, Connelly A. *Unsupervised 3-tissue response function estimation from single-shell or multi-shell diffusion MR data without a co-registered T1 image*. ISMRM Workshop on Breaking the Barriers of Diffusion MRI 5; 2016.
- Frassle S, Lomakina EI, Razi A, Friston KJ, Buhmann JM, Stephan KE. Regression DCM for fMRI. *NeuroImage*. 2017;155:406–421.
- Freyer F, Roberts JA, Becker R, Robinson PA, Ritter P, Breakspear M. Biophysical mechanisms of multistability in resting-state cortical rhythms. *J Neurosci*. 2011;31(17):6353–6361.
- Freyer F, Roberts JA, Ritter P, Breakspear M. A canonical model of multistability and scale-invariance in biological systems. *PLoS Comput Biol*. 2012;8(8):e1002634.
- Friston K. Causal modelling and brain connectivity in functional magnetic resonance imaging. *PLoS Biol*. 2009;7(2):e33.
- Funahashi S, Bruce CJ, Goldman-Rakic PS. Mnemonic coding of visual space in monkey dorsolateral prefrontal cortex. *J Neurophysiol*. 1989;61(2):331–349.
- Funahashi S, Bruce CJ, Goldman-Rakic PS. Dorsolateral prefrontal lesions and oculomotor delayed-response performance: evidence for mnemonic "scotomas". *J Neurosci*. 1993;13(4):1479–1497.

- Fuster JM. *The prefrontal cortex*. London: Academic Press; 2015.
- Fuster JM. Cognitive networks (Cognits) process and maintain working memory. *Front Neural Circuits*. 2021;15:790691.
- Germann J, Petrides M. Area 8A within the posterior middle frontal gyrus underlies cognitive selection between competing visual targets. *eNeuro*. 2020a;7(5). <https://doi.org/10.1523/ENEURO.0102-1520>.
- Germann J, Petrides M. The ventral part of dorsolateral frontal area 8A regulates visual attentional selection and the dorsal part auditory attentional selection. *Neuroscience*. 2020b;441:209–216.
- Gilson M, Moreno-Bote R, Ponce-Alvarez A, Ritter P, Deco G. Estimation of directed effective connectivity from fMRI functional connectivity hints at asymmetries in the cortical connectome. *PLoS Comput Biol*. 2016;12(3):e1004762.
- Glasser MF, Sotiropoulos SN, Wilson JA, Coalson TS, Fischl B, Andersson JL, Xu J, Jbabdi S, Webster M, Polimeni JR, et al. The minimal preprocessing pipelines for the human connectome project. *NeuroImage*. 2013;80:105–124.
- Glasser MF, Coalson TS, Robinson EC, Hacker CD, Harwell J, Yacoub E, Ugurbil K, Andersson J, Beckmann CF, Jenkinson M, et al. A multi-modal parcellation of human cerebral cortex. *Nature*. 2016a;536(7615):171–178.
- Glasser MF, Smith SM, Marcus DS, Andersson JL, Auerbach EJ, Behrens TE, Coalson TS, Harms MP, Jenkinson M, Moeller S, et al. The human connectome Project's neuroimaging approach. *Nat Neurosci*. 2016b;19(9):1175–1187.
- Goldman-Rakic PS. The prefrontal landscape: implications of functional architecture for understanding human mentation and the central executive. *Philos Trans R Soc B*. 1996;351(1346):1445–1453.
- Goldman-Rakic PS, Leung H-C. Functional architecture of the dorsolateral prefrontal cortex in monkeys and humans. In: Stuss DT, Knight RT, editors. *Principles of frontal lobe function*. New York: Oxford University Press; 2002. pp. 85–95.
- Goulas A, Stiers P, Hutchison RM, Everling S, Petrides M, Margulies DS. Intrinsic functional architecture of the macaque dorsal and ventral lateral frontal cortex. *J Neurophysiol*. 2017;117(3):1084–1099.
- Grabenhorst F, Rolls ET. Value, pleasure, and choice in the ventral prefrontal cortex. *Trends Cogn Sci*. 2011;15(2):56–67.
- Griffanti L, Salimi-Khorshidi G, Beckmann CF, Auerbach EJ, Douaud G, Sexton CE, Zsoldos E, Ebmeier KP, Filippini N, Mackay CE, et al. ICA-based artefact removal and accelerated fMRI acquisition for improved resting state network imaging. *NeuroImage*. 2014;95:232–247.
- Hanlon CA, Czoty PW, Smith HR, Epperly PM, Galbo LK. Cortical excitability in a nonhuman primate model of TMS. *Brain Stimul*. 2021;14(1):19–21.
- Hogeveen J, Medalla M, Ainsworth M, Galeazzi JM, Hanlon CA, Mansouri FA, Costa VD. What does the frontopolar cortex contribute to goal-directed cognition and action? *J Neurosci*. 2022a;42(45):8508–8513.
- Hogeveen J, Mullins TS, Romero JD, Eversole E, Rogge-Obando K, Mayer AR, Costa VD. The neurocomputational bases of explore-exploit decision-making. *Neuron*. 2022b;110:1869–1879.e5.
- Huang C-C, Rolls ET, Hsu C-CH, Feng J, Lin C-P. Extensive cortical connectivity of the human hippocampal memory system: beyond the "what" and "where" dual-stream model. *Cereb Cortex*. 2021;31(10):4652–4669.
- Huang CC, Rolls ET, Feng J, Lin CP. An extended human connectome project multimodal parcellation atlas of the human cortex and subcortical areas. *Brain Struct Funct*. 2022;227(3):763–778.
- Jeurissen B, Tournier JD, Dhollander T, Connelly A, Sijbers J. Multi-tissue constrained spherical deconvolution for improved analysis of multi-shell diffusion MRI data. *NeuroImage*. 2014;103:411–426.
- Kelly C, Uddin LQ, Shehzad Z, Margulies DS, Castellanos FX, Milham MP, Petrides M. Broca's region: linking human brain functional connectivity data and non-human primate tracing anatomy studies. *Eur J Neurosci*. 2010;32(3):383–398.
- Kringelbach ML, Deco G. Brain states and transitions: insights from computational neuroscience. *Cell Rep*. 2020;32(10):108128.
- Kringelbach ML, O'Doherty J, Rolls ET, Andrews C. Activation of the human orbitofrontal cortex to a liquid food stimulus is correlated with its subjective pleasantness. *Cereb Cortex*. 2003;13(10):1064–1071.
- Kringelbach ML, McIntosh AR, Ritter P, Jirsa VK, Deco G. The rediscovery of slowness: exploring the timing of cognition. *Trends Cogn Sci*. 2015;19(10):616–628.
- Kuznetsov YA. *Elements of applied bifurcation theory*. New York: Springer Science and Business Media; 2013.
- Lundqvist M, Herman P, Miller EK. Working memory: delay activity, yes! Persistent activity? Maybe not. *J Neurosci*. 2018;38(32):7013–7019.
- Ma Q, Rolls ET, Huang C-C, Cheng W, Feng J. Extensive cortical functional connectivity of the human hippocampal memory system. *Cortex*. 2022;147:83–101.
- Maier-Hein KH, Neher PF, Houde JC, Cote MA, Garyfallidis E, Zhong J, Chamberland M, Yeh FC, Lin YC, Ji Q, et al. The challenge of mapping the human connectome based on diffusion tractography. *Nat Commun*. 2017;8(1):1349.
- Mansouri FA, Egner T, Buckley MJ. Monitoring demands for executive control: shared functions between human and nonhuman primates. *Trends Neurosci*. 2017a;40(1):15–27.
- Mansouri FA, Koechlin E, Rosa MGP, Buckley MJ. Managing competing goals - a key role for the frontopolar cortex. *Nat Rev Neurosci*. 2017b;18(11):645–657.
- Markov NT, Ersey-Ravasz MM, Ribeiro Gomes AR, Lamy C, Magrou L, Vezoli J, Misery P, Falchier A, Quilodran R, Gariel MA, et al. A weighted and directed interareal connectivity matrix for macaque cerebral cortex. *Cereb Cortex*. 2014;24(1):17–36.
- Martinez-Garcia M, Rolls ET, Deco G, Romo R. Neural and computational mechanisms of postponed decisions. *Proc Natl Acad Sci USA*. 2011;108(28):11626–11631.
- Medalla M, Barbas H. Anterior cingulate synapses in prefrontal areas 10 and 46 suggest differential influence in cognitive control. *J Neurosci*. 2010;30(48):16068–16081.
- Medalla M, Barbas H. Specialized prefrontal "auditory fields": organization of primate prefrontal-temporal pathways. *Front Neurosci*. 2014;8:77.
- Miller EK. The "working" of working memory. *Dialogues Clin Neurosci*. 2013;15(4):411–418.
- Miller EK, Lundqvist M, Bastos AM. Working memory 2.0. *Neuron*. 2018;100(2):463–475.
- Pandya DN, Seltzer B, Petrides M, Cipolloni PB. *Cerebral cortex: architecture, connections, and the dual origin concept*. New York: Oxford University Press; 2015.
- Passingham RE. *Understanding the prefrontal cortex: selective advantage, connectivity and neural operations*. Oxford: Oxford University Press; 2021.
- Petrides M. *Neuroanatomy of language regions of the human brain*. New York: Academic Press; 2014.
- Petrides M, Pandya DN. Dorsolateral prefrontal cortex: comparative cytoarchitectonic analysis in the human and the macaque brain and corticocortical connection patterns. *Eur J Neurosci*. 1999;11(3):1011–1036.

- Petrides M, Tomaiuolo F, Yeterian EH, Pandya DN. The prefrontal cortex: comparative architectonic organization in the human and the macaque monkey brains. *Cortex*. 2012;48(1):46–57.
- Power JD, Cohen AL, Nelson SM, Wig GS, Barnes KA, Church JA, Vogel AC, Laumann TO, Miezin FM, Schlaggar BL, et al. Functional network organization of the human brain. *Neuron*. 2011;72(4):665–678.
- Rajalingham R, Issa EB, Bashivan P, Kar K, Schmidt K, DiCarlo JJ. Large-scale, high-resolution comparison of the core visual object recognition behavior of humans, monkeys, and state-of-the-art deep artificial neural networks. *J Neurosci*. 2018;38(33):7255–7269.
- Razi A, Seghier ML, Zhou Y, McColgan P, Zeidman P, Park HJ, Sporns O, Rees G, Friston KJ. Large-scale DCMs for resting-state fMRI. *Netw Neurosci*. 2017;1(3):222–241.
- Renart A, Moreno R, de la Rocha J, Parga N, Rolls ET. A model of the IT-PF network in object working memory which includes balanced persistent activity and tuned inhibition. *Neurocomputing*. 2001;38-40:1525–1531.
- Rojkova K, Volle E, Urbanski M, Humbert F, Dell'Acqua F, Thiebaut de Schotten M. Atlas of the frontal lobe connections and their variability due to age and education: a spherical deconvolution tractography study. *Brain Struct Funct*. 2016;221(3):1751–1766.
- Rolls ET. Functions of the primate temporal lobe cortical visual areas in invariant visual object and face recognition. *Neuron*. 2000;27(2):205–218.
- Rolls ET. *Cerebral cortex: principles of operation*. Oxford: Oxford University Press; 2016a.
- Rolls ET. Reward systems in the brain and nutrition. *Annu Rev Nutr*. 2016b;36(1):435–470.
- Rolls ET. The storage and recall of memories in the hippocampocortical system. *Cell Tissue Res*. 2018;373(3):577–604.
- Rolls ET. The orbitofrontal cortex and emotion in health and disease, including depression. *Neuropsychologia*. 2019;128:14–43.
- Rolls ET. *Brain computations: what and how*. Oxford: Oxford University Press; 2021a.
- Rolls ET. The connections of neocortical pyramidal cells can implement the learning of new categories, attractor memory, and top-down recall and attention. *Brain Struct Funct*. 2021b;226(8):2523–2536.
- Rolls ET. Learning invariant object and spatial view representations in the brain using slow unsupervised learning. *Front Comput Neurosci*. 2021c;15:686239.
- Rolls ET. Mind causality: a computational neuroscience approach. *Front Comput Neurosci*. 2021d;15:70505.
- Rolls ET. The hippocampus, ventromedial prefrontal cortex, and episodic and semantic memory. *Prog Neurobiol*. 2022;217:102334.
- Rolls ET. *Brain computations and connectivity*. Oxford: Oxford University Press. Open Access; 2023a.
- Rolls ET. Emotion, motivation, decision-making, the orbitofrontal cortex, anterior cingulate cortex, and the amygdala. *Brain Struct Funct*. 2023b;228(5):1201–1257.
- Rolls ET. Hippocampal spatial view cells for memory and navigation, and their underlying connectivity in humans. *Hippocampus*. 2023c;33(5):533–572.
- Rolls ET, Murzi E, Yaxley S, Thorpe SJ, Simpson SJ. Sensory-specific satiety: food-specific reduction in responsiveness of ventral fore-brain neurons after feeding in the monkey. *Brain Res*. 1986;368(1):79–86.
- Rolls ET, Sienkiewicz ZJ, Yaxley S. Hunger modulates the responses to gustatory stimuli of single neurons in the caudolateral orbitofrontal cortex of the macaque monkey. *Eur J Neurosci*. 1989;1(1):53–60.
- Rolls ET, Vatansever D, Li Y, Cheng W, Feng J. Rapid rule-based reward reversal and the lateral orbitofrontal cortex. *Cereb Cortex Commun*. 2020;1(1):tgaa087.
- Rolls ET, Deco G, Huang C-C, Feng J. The human language effective connectome. *NeuroImage*. 2022a;258:119352.
- Rolls ET, Deco G, Huang CC, Feng J. The effective connectivity of the human hippocampal memory system. *Cereb Cortex*. 2022b;32(17):3706–3725.
- Rolls ET, Deco G, Huang C-C, Feng J. Human amygdala compared to orbitofrontal cortex connectivity, and emotion. *Prog Neurobiol*. 2023a;220:102385.
- Rolls ET, Deco G, Huang C-C, Feng J. Multiple cortical visual streams in humans. *Cereb Cortex*. 2023b;33(7):3319–3349.
- Rolls ET, Deco G, Huang CC, Feng J. The human orbitofrontal cortex, vmPFC, and anterior cingulate cortex effective connectome: emotion, memory, and action. *Cereb Cortex*. 2023c;33:330–359.
- Rolls ET, Deco G, Huang CC, Feng J. The human posterior parietal cortex: effective connectome, and its relation to function. *Cereb Cortex*. 2023d;33(6):3142–3170.
- Rolls ET, Deco G, Huang CC, Feng J. Prefrontal and somatosensory-motor cortex effective connectivity in humans. *Cereb Cortex*. 2023e;33(8):4939–4963.
- Rolls ET, Deco G, Zhang Y, Feng J. Hierarchical organisation of the human ventral visual streams revealed with magnetoencephalography. *Cereb Cortex*. 2023f;33(20):10686–10701.
- Rolls ET, Rauschecker JP, Deco G, Huang CC, Feng J. Auditory cortical connectivity in humans. *Cereb Cortex*. 2023g;33(10):6207–6227.
- Rolls ET, Wirth S, Deco G, Huang C-C, Feng J. The human posterior cingulate, retrosplenial and medial parietal cortex effective connectome, and implications for memory and navigation. *Hum Brain Mapp*. 2023h;44(2):629–655.
- Salimi-Khorshidi G, Douaud G, Beckmann CF, Glasser MF, Griffanti L, Smith SM. Automatic denoising of functional MRI data: combining independent component analysis and hierarchical fusion of classifiers. *NeuroImage*. 2014;90:449–468.
- Sallet J, Mars RB, Noonan MP, Neubert FX, Jbabdi S, O'Reilly JX, Filippini N, Thomas AG, Rushworth MF. The organization of dorsal frontal cortex in humans and macaques. *J Neurosci*. 2013;33(30):12255–12274.
- Satterthwaite TD, Elliott MA, Gerraty RT, Ruparel K, Loughhead J, Calkins ME, Eickhoff SB, Hakonarson H, Gur RC, Gur RE, et al. An improved framework for confound regression and filtering for control of motion artifact in the preprocessing of resting-state functional connectivity data. *NeuroImage*. 2013;64:240–256.
- Scheirer J, Ray WS, Hare N. The analysis of ranked data derived from completely randomized factorial designs. *Biometrics*. 1976;32(2):429–434.
- Schmahmann JD, Pandya DN. *Fiber pathways of the brain*. Oxford: Oxford University Press; 2006.
- Shallice T, Burgess PW. Deficits in strategy application following frontal lobe damage in man. *Brain*. 1991;114(Pt 2):727–741.
- Shallice T, Cipolotti L. The prefrontal cortex and neurological impairments of active thought. *Annu Rev Psychol*. 2018;69(1):157–180.
- Sinha N. Non-parametric alternative of 2-way ANOVA (ScheirerRayHare) MATLAB central file exchange, <https://www.mathworks.com/matlabcentral/fileexchange/96399-non-parametric-alternative-of-96392-way-anova-scheirerrayahare>. 2022.
- Smith SM. Fast robust automated brain extraction. *Hum Brain Mapp*. 2002;17(3):143–155.
- Smith SM, Beckmann CF, Andersson J, Auerbach EJ, Bijsterbosch J, Douaud G, Duff E, Feinberg DA, Griffanti L, Harms MP, et al.

- Resting-state fMRI in the human connectome project. *NeuroImage*. 2013;80:144–168.
- Smith RE, Tournier JD, Calamante F, Connelly A. SIFT2: enabling dense quantitative assessment of brain white matter connectivity using streamlines tractography. *NeuroImage*. 2015;119:338–351.
- Sulpizio V, Galati G, Fattori P, Galletti C, Pitzalis S. A common neural substrate for processing scenes and egomotion-compatible visual motion. *Brain Struct Funct*. 2020;225(7):2091–2110.
- Thiebaut de Schotten M, Dell'Acqua F, Valabregue R, Catani M. Monkey to human comparative anatomy of the frontal lobe association tracts. *Cortex*. 2012;48(1):82–96.
- Treves A, Rolls ET. A computational analysis of the role of the hippocampus in memory. *Hippocampus*. 1994;4(3):374–391.
- Valdes-Sosa PA, Roebroek A, Daunizeau J, Friston K. Effective connectivity: influence, causality and biophysical modeling. *NeuroImage*. 2011;58(2):339–361.
- Van Essen DC, Smith SM, Barch DM, Behrens TE, Yacoub E, Ugurbil K, Consortium WU-MH. The WU-Minn human connectome project: an overview. *NeuroImage*. 2013;80:62–79.
- Van Essen DC, Glasser MF. Parcellating cerebral cortex: how invasive animal studies inform noninvasive mapmaking in humans. *Neuron*. 2018;99(4):640–663.
- Yeterian EH, Pandya DN, Tomaiuolo F, Petrides M. The cortical connectivity of the prefrontal cortex in the monkey brain. *Cortex*. 2012;48(1):58–81.
- Yokoyama C, Autio JA, Ikeda T, Sallet J, Mars RB, Van Essen DC, Glasser MF, Sadato N, Hayashi T. Comparative connectomics of the primate social brain. *NeuroImage*. 2021;245:118693.
- Zhuang C, Yan S, Nayebi A, Schrimpf M, Frank MC, DiCarlo JJ, Yamins DLK. Unsupervised neural network models of the ventral visual stream. *Proc Natl Acad Sci USA*. 2021;118(3):e2014196118.